

Transient Photoactivation of Anionophores by Using Redshifted Fast-Relaxing Azobenzenes

Aidan Kerckhoffs, Manzoor Ahmad and Matthew J. Langton*

Contents

1 Materials and methods	2
2 Synthesis and Characterisation	3
3 Photo-switching: Half-Life Determination and UV-Vis spectra	12
4 Anion transport studies	16
5 References.....	25

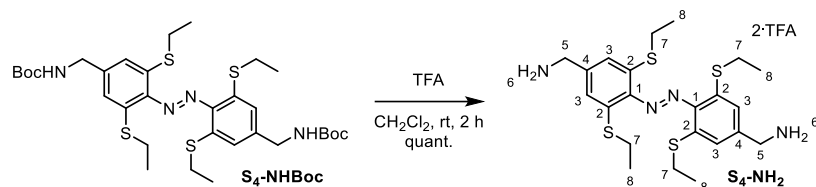
1 Materials and methods

All reagents and solvents were purchased from commercial sources and used without further purification. Lipids were purchased from Avanti Polar Lipids and used without further purification. Where necessary, solvents were dried by passing through an MBraun MPSP-800 column and degassed with nitrogen. Triethylamine was distilled from and stored over potassium hydroxide. Column chromatography was carried out on Merck® silica gel 60 under a positive pressure of nitrogen. Where mixtures of solvents were used, ratios are reported by volume. NMR spectra were recorded on a Bruker AVIII 400, Bruker AVII 500 (with cryoprobe) and Bruker AVIII 500 spectrometers. Chemical shifts are reported as δ values in ppm. Mass spectra were carried out on a Waters Micromass LCT and Bruker microTOF spectrometers. Fluorescence spectroscopic data were recorded using a Horiba Duetta fluorescence spectrophotometer, equipped with Peltier temperature controller and stirrer. UV-Vis spectra were recorded on a V-770 UV-Visible/NIR Spectrophotometer equipped with Peltier temperature controller and stirrer using quartz cuvettes of 1 cm path length. Experiments were conducted at 25°C unless otherwise stated. Vesicles were prepared as described below using Avestin “LiposoFast” extruder apparatus, equipped with polycarbonate membranes with 200 nm pores. GPC purification of vesicles was carried out using GE Healthcare PD-10 desalting columns prepacked with Sephadex G 25 medium.

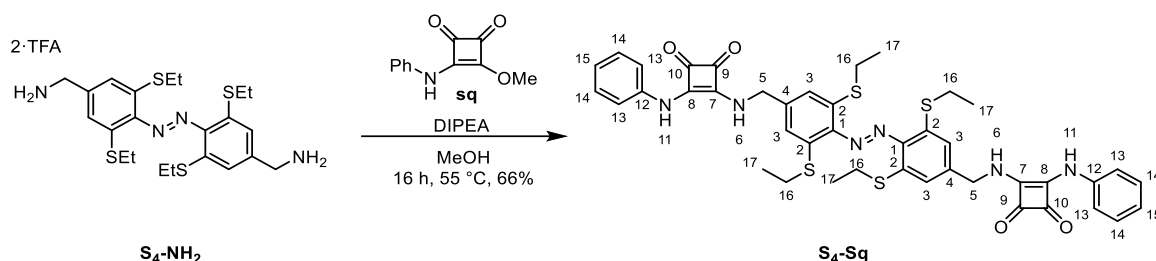
Abbreviations

Boc: tert-butyloxycarbonyl; CF: 5(6)-Carboxyfluorescein; DBU: 1,8-Diazabicyclo[5.4.0]undec-7-ene; DCM: Dichloromethane; DIPEA: N,N-Diisopropylethylamine; DMF: N,N-Dimethylformamide; DMSO: Dimethylsulfoxide; DPPC: 1,2-dipalmitoyl-sn-glycero-3-phosphocholine; EYPG: egg-yolk phosphatidylglycerol; HEPES: N-(2-hydroxyethyl)piperazine-N'-(2-ethanesulfonic acid); HPTS: 8-hydroxy-1,3,6-pyrenetrisulfonate; HRMS: High resolution mass spectrometry; KF: Potassium Fluoride; KOH: Potassium hydroxide; LUVs: large unilamellar vesicles; MeCN: Acetonitrile; MeOH: Methanol; NCS: N-Chlorosuccinimide; POPC: 1-palmitoyl-2-oleoyl-sn-glycero-3-phosphocholine; PSS: Photostationary State; rt: Room temperature; TFA: Trifluoroacetic acid; THF: Tetrahydrofuran.

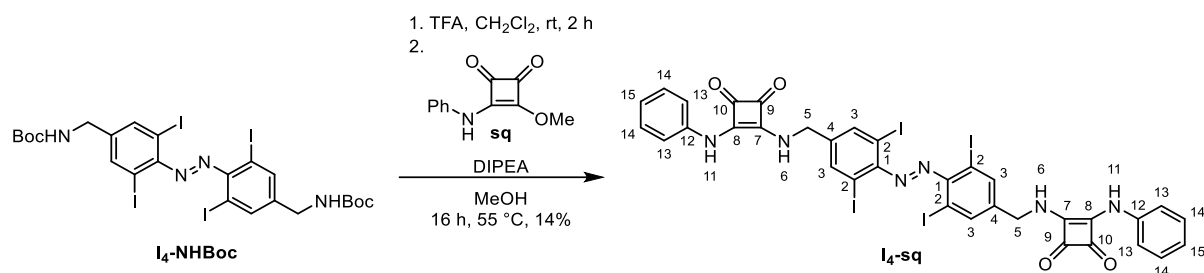
2 Synthesis and Characterisation



To a solution of **S₄-NHBoc**¹ (70.0 mg, 103 μmol) in CH₂Cl₂ (1.50 mL) was added TFA (180 μL). The reaction was stirred at room temperature for 2 hours. The TFA was removed under a stream of nitrogen, then dried in vacuo to afford the title compound as an orange solid (73.0 mg, 103 μmol, 100%) **E-S₄-NH₂**: ¹H NMR (400 MHz, MeOD) δ 7.32 (s, 4H, H-3), 4.19 (s, 4H, H-5), 2.98 (q, *J* = 7.4 Hz, 8H, H-7), 1.32 (t, *J* = 7.4 Hz, 12H, H-8). ¹³C NMR (126 MHz, MeOD) δ 148.08 (C-1), 138.88 (C-2), 135.79 (C-4), 123.87 (C-3), 44.05 (C-5), 27.64 (C-7), 13.78 (C-8). HRMS-EI (*m/z*) Calculated for C₂₂H₃₃N₄S₄ [M+H]⁺, 481.1583; found 481.1578



S₄-NH₂ (39.0 mg, 55.0 μmol) was dissolved in MeOH (1.00 mL). DIPEA (580 μL, 0.330 mmol, 6 eq) was added dropwise. Monosquaramide **sq**² (22.4 mg, 110 μmol, 2 eq) in MeCN (1mL) was added, and the solution was heated at 55 °C for 16 hours. The reaction was cooled to rt and the solid precipitate was filtered and washed sequentially with MeOH and MeCN, then collected and dried under high vacuum to afford the title compound as an orange solid (30.0 mg, 36.5 μmol, 66%). **E-S₄-sq**: ¹H NMR (500 MHz, DMSO) δ 9.75 (s, 2H, H-11), 8.12 (s, 2H, H-6), 7.43 (d, *J* = 8.0 Hz, 4H, H-13), 7.37 – 7.32 (m, 4H, H-14), 7.27 (s, 4H, H-3), 7.04 (tt, *J* = 7.3, 1.2 Hz, 2H, H-15), 4.84 (s, 4H, H-5), 2.91 (q, *J* = 7.4 Hz, 8H, H-16), 1.20 (t, *J* = 7.3 Hz, 12H, H-17). ¹³C NMR (126 MHz, DMSO) δ 184.51 (C-10), 180.60 (C-9), 168.90 (C-8), 164.25 (C-7), 145.13 (C-1), 140.42 (C-4), 138.88 (C-12), 136.27 (C-2), 129.36 (C-14), 122.82 (C-15), 121.34 (C-3), 118.20 (C-13), 46.96 (C-5), 25.66 (C-16), 13.35 (C-17). HRMS-EI (*m/z*) Calculated for C₄₂H₄₁O₄N₆S₄ [M+H]⁺, 821.2078; found 821.2072



I₄-sq. To a solution of **I₄-NH₂Boc**¹ (32.0 mg, 34.0 μmol) in CH₂Cl₂ (2.00 mL) was added TFA (0.20 mL). The reaction was stirred at rt for 2 h. The TFA and solvent were removed by evaporation under a stream of nitrogen and then under high vacuum. The crude diamine was dissolved in MeOH (0.5 mL). DIPEA (30.0 μL) was added dropwise. Monosquaramide **sq²** (13.8 mg, 68.0 μmol, 2.00 eq) in MeCN (0.500 mL) was added, and the solution was heated at 40 °C for 16 hours. The reaction was cooled to rt and the solid precipitate was filtered and washed sequentially with MeOH and MeCN, then collected and dried under high vacuum to afford the title compound as a purple solid (6.04 mg, 4.80 μmol, 14%).

E-S₄-sq: ¹H NMR (600 MHz, DMSO) δ 9.75 (s, 2H, H-11), 8.12 (d, *J* = 5.8 Hz, 4H, H-3), 8.09 – 8.01 (m, 2H, H-6), 7.43 (d, *J* = 7.9 Hz, 4H, H-13), 7.37 – 7.32 (m, 4H, H-14), 7.04 (tt, *J* = 7.3, 1.2 Hz, 2H, H-15), 4.82 (d, *J* = 5.2 Hz, 4H, H-5). ¹³C NMR (151 MHz, DMSO) δ 184.01 (C-10), 180.68 (C-9), 168.65 (C-8), 164.15 (C-7), 149.43 (C-1), 143.07 (C-4), 139.77 (C-3), 138.85 (C-12), 129.29 (C-14), 122.77 (C-15), 118.21 (C-13), 91.25 (C-2), 45.21 (C-5). HRMS-EI (*m/z*) Calculated for C₃₄H₂₃N₆O₄I₄ [M+H]⁺, 1086.7954; found 1086.7954.

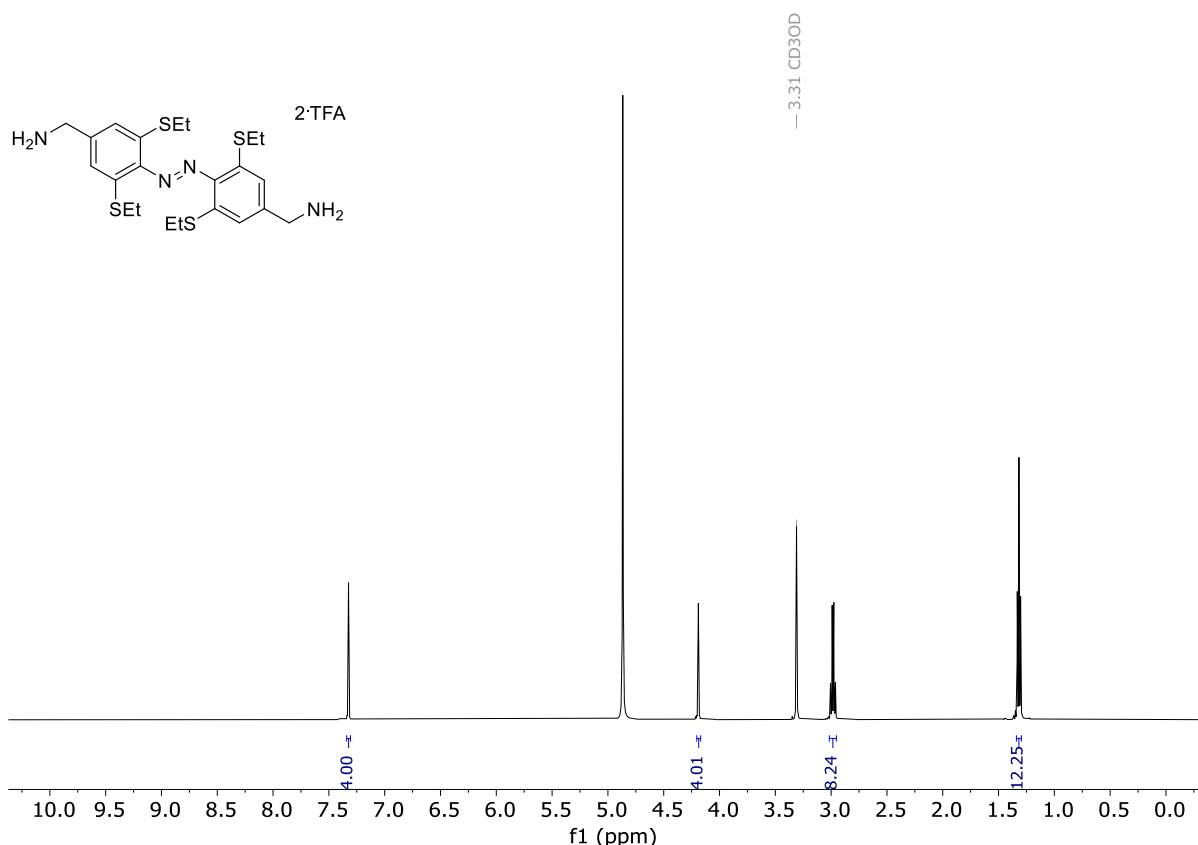


Figure S1. ¹H NMR Spectrum of **S₄-NH₂** (MeOD-*d*₄, 298 K).

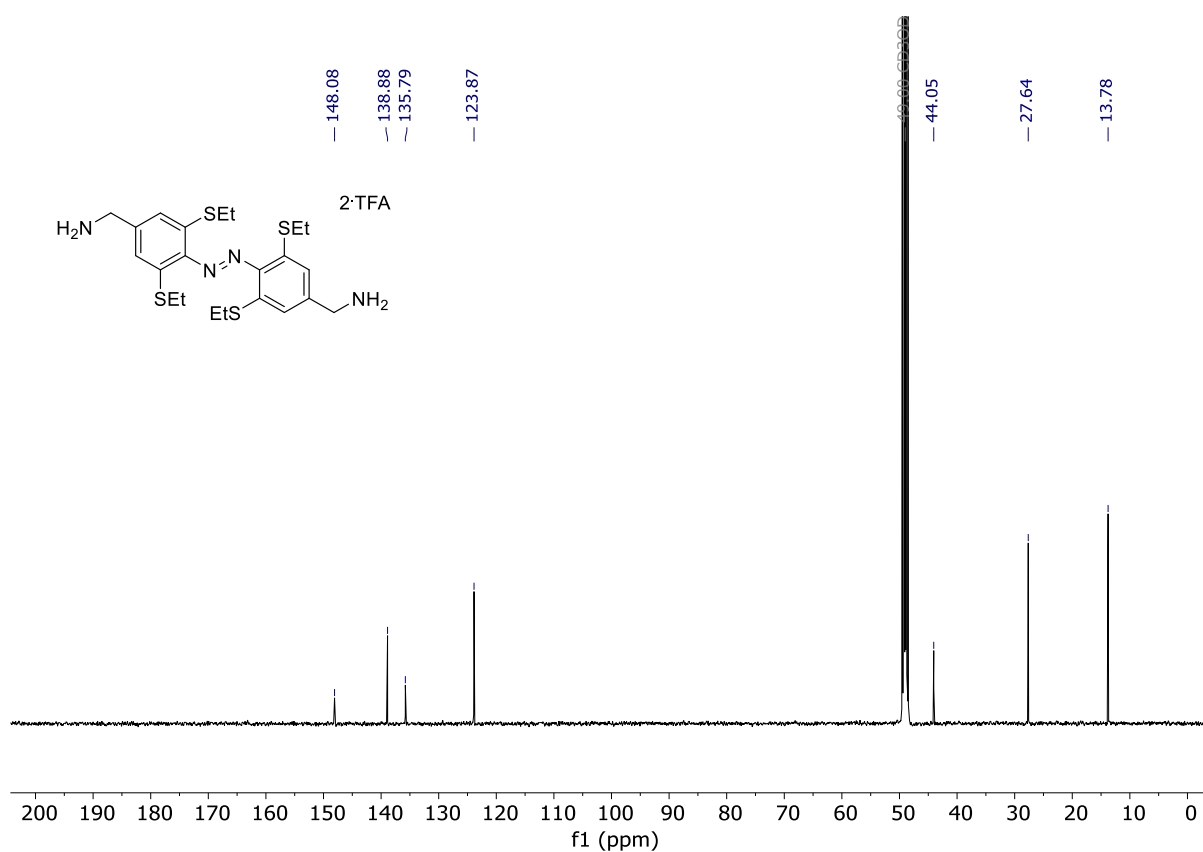


Figure S2. ¹³C NMR Spectrum of **S₄-NH₂** (MeOD-*d*₄, 298 K).

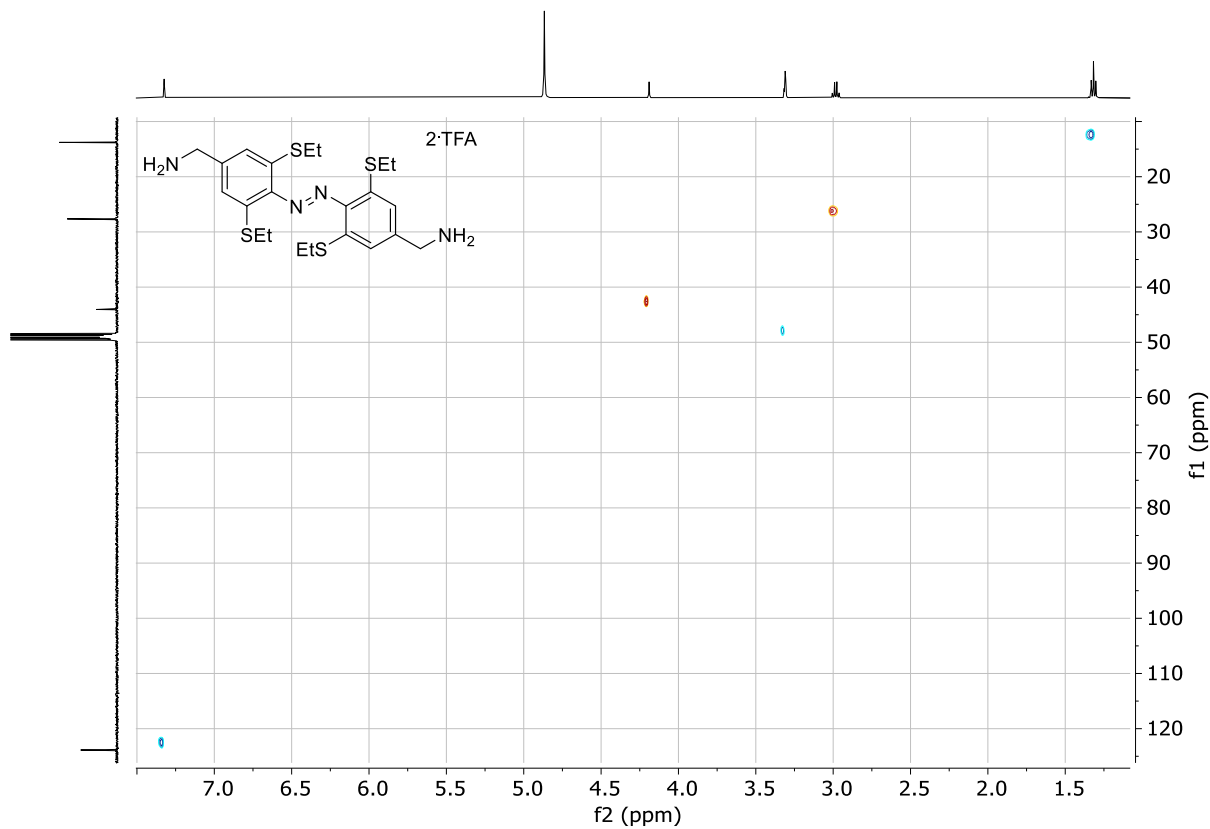


Figure S3. HSQC NMR Spectrum of **S₄-NH₂** (MeOD-*d*₄, 298 K).

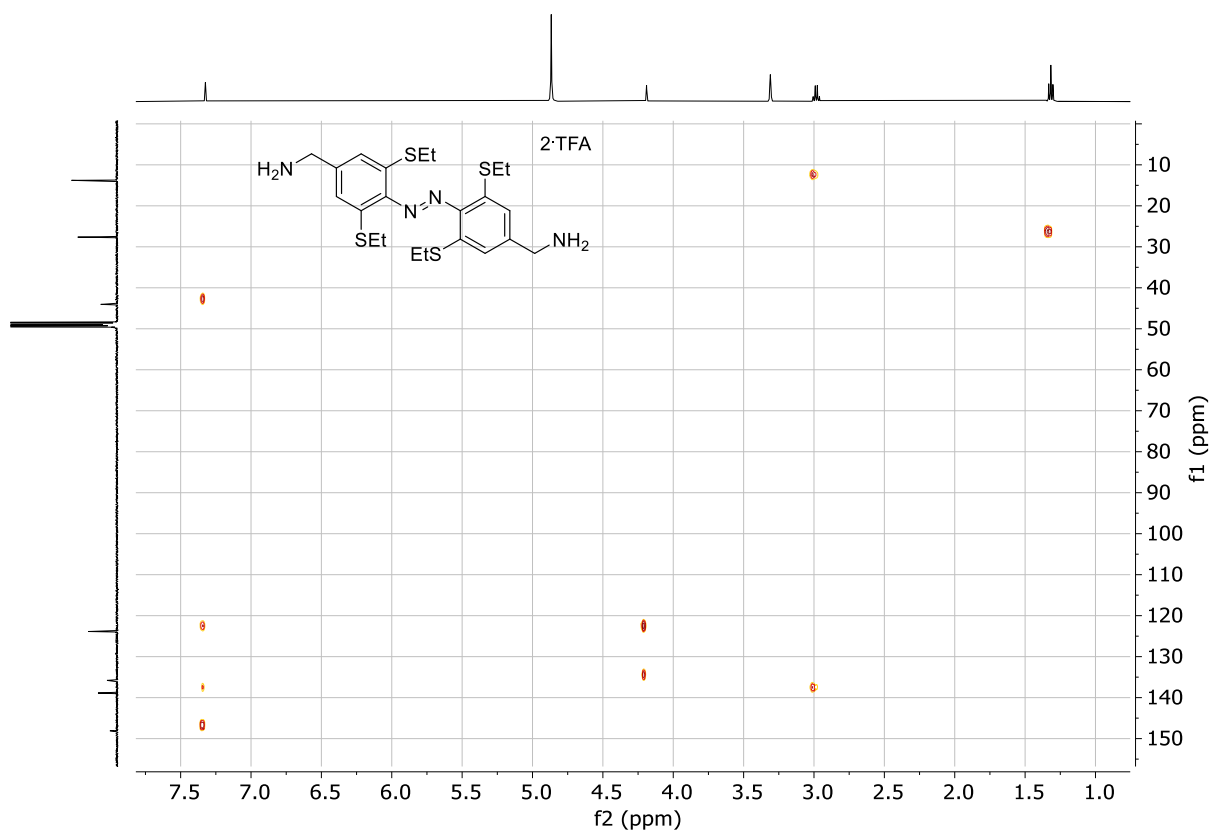


Figure S4. HMBC NMR Spectrum of **S₄-NH₂** (MeOD-*d*₄, 298 K).

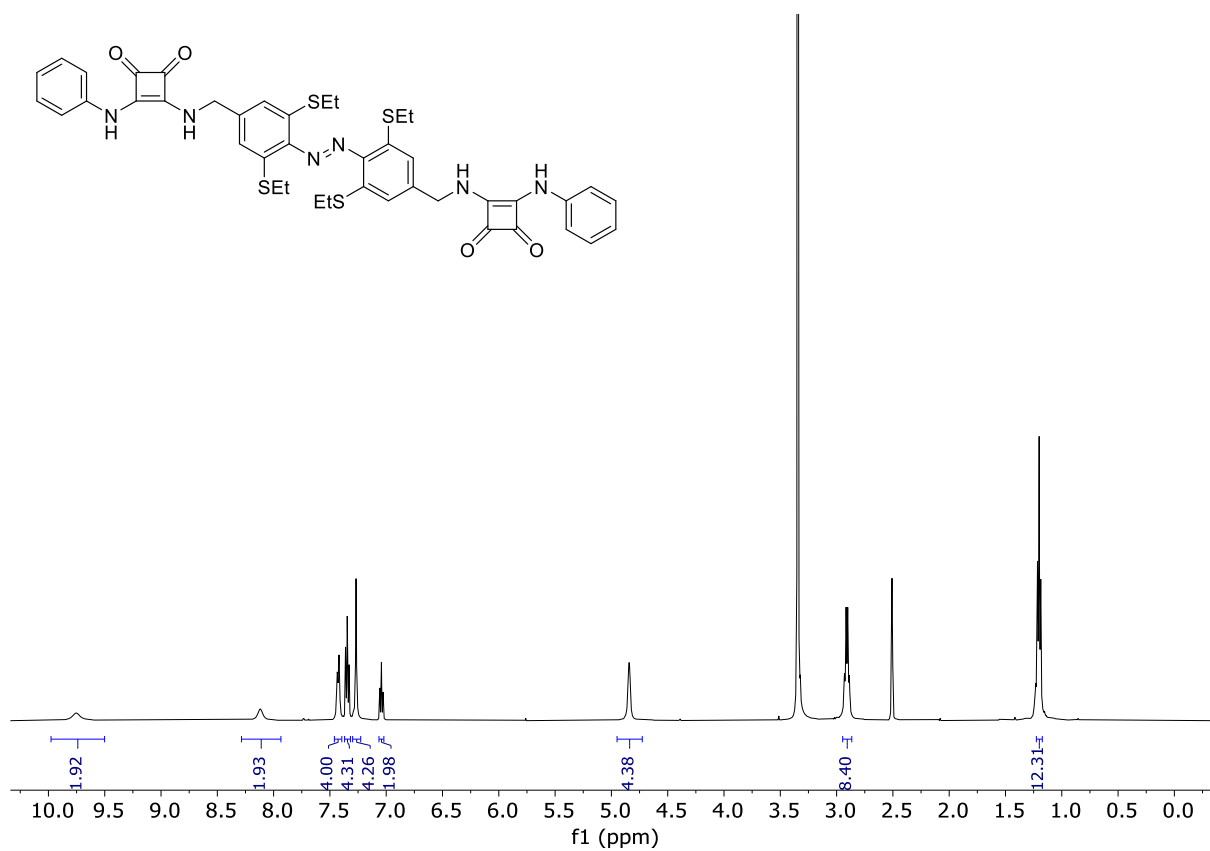


Figure S5. ¹H NMR Spectrum of **S₄-sq** (DMSO-*d*₆, 298 K).

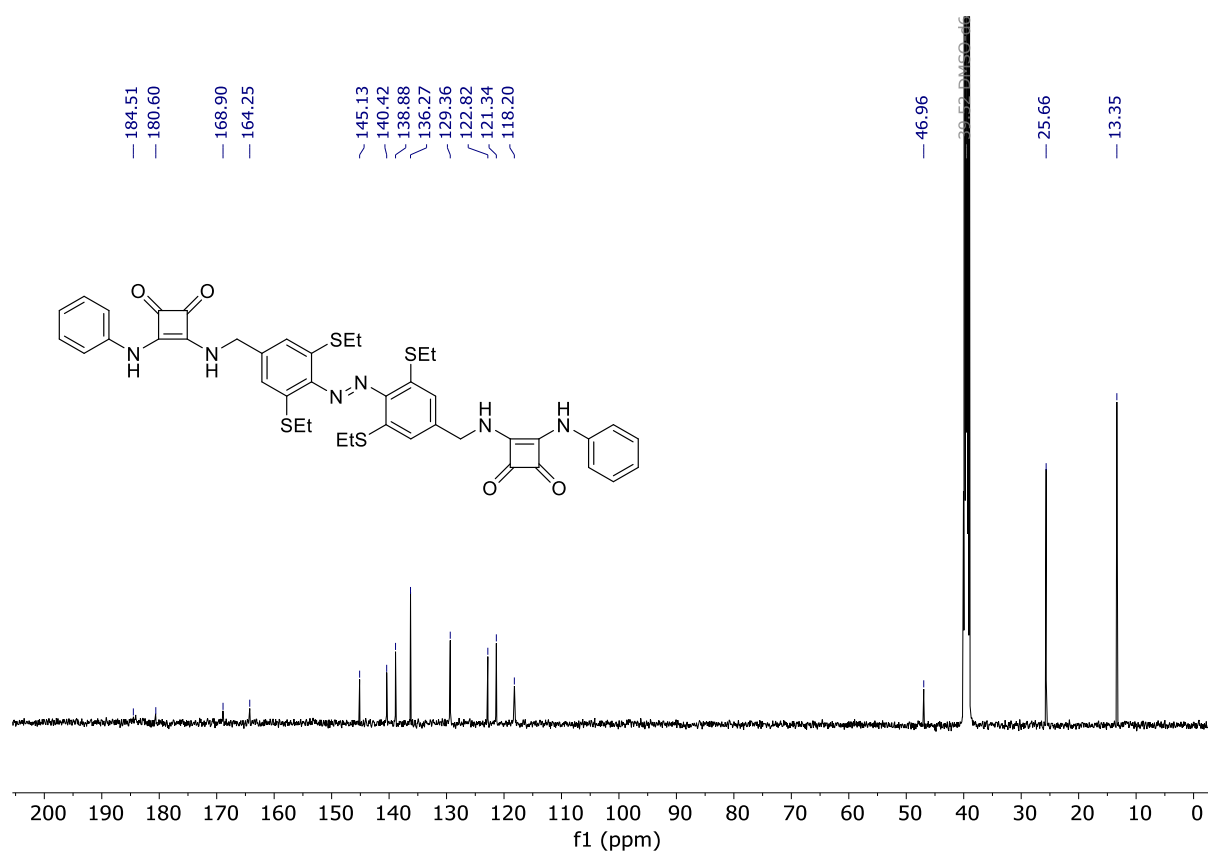


Figure S6. ¹³C NMR Spectrum of **S₄-sq** (DMSO-*d*₆, 298 K).

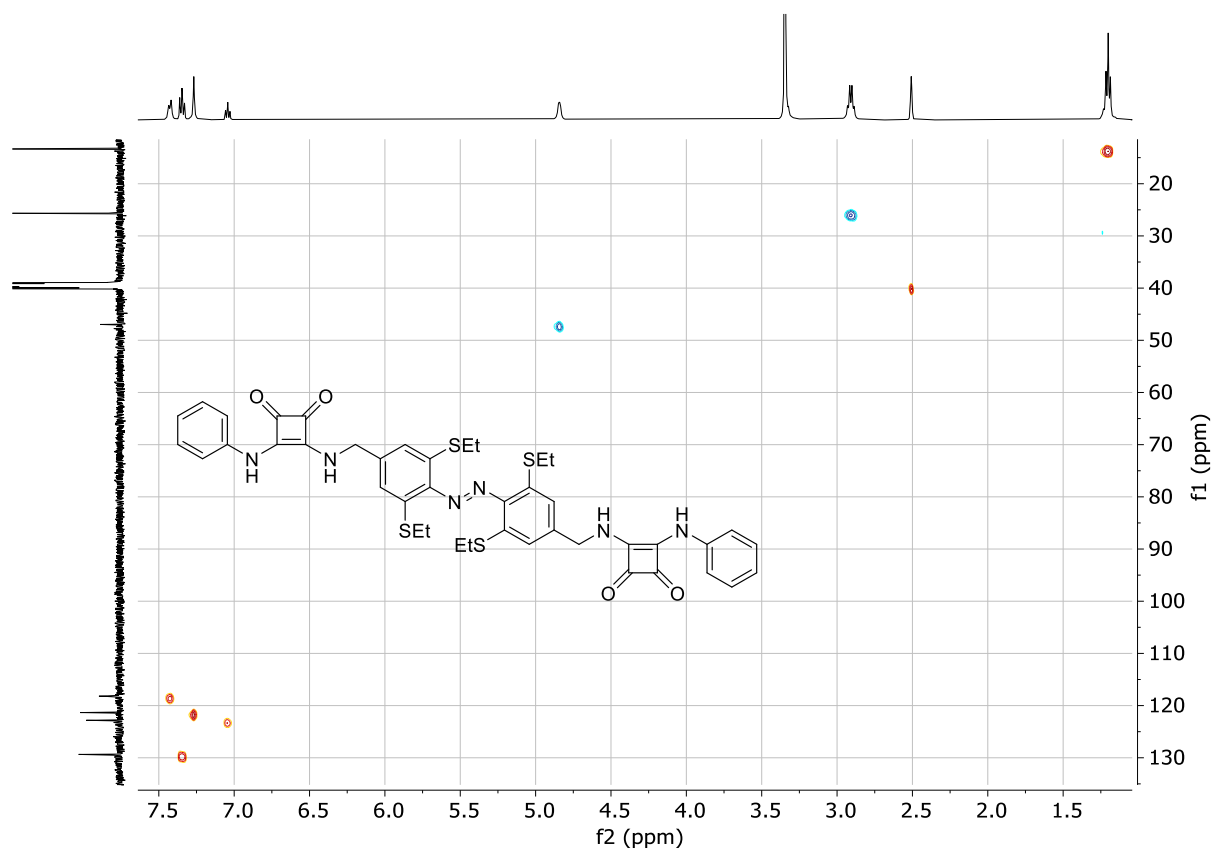


Figure S7. HSQC NMR Spectrum of **S₄-sq** (DMSO-*d*₆, 298 K).

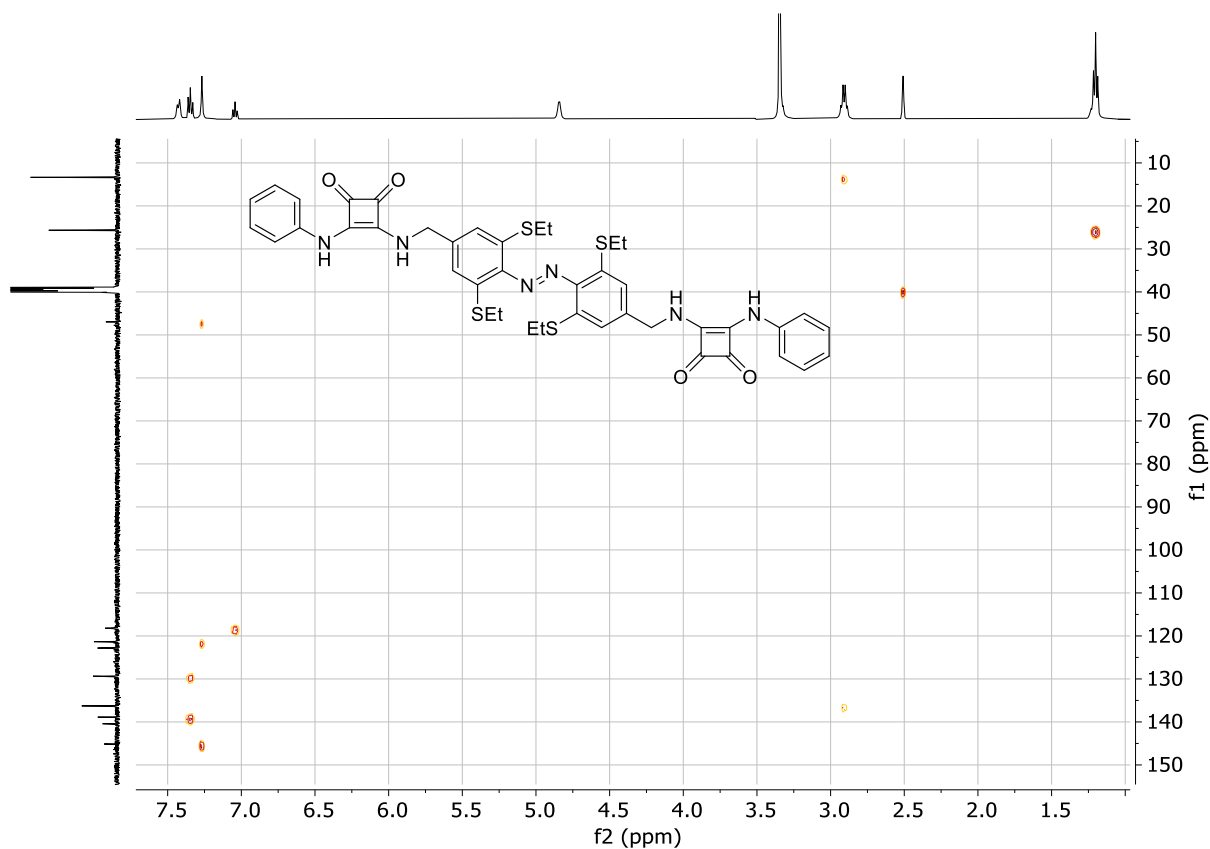


Figure S8. HMBC NMR Spectrum of **S4-sq** (DMSO- d_6 , 298 K).

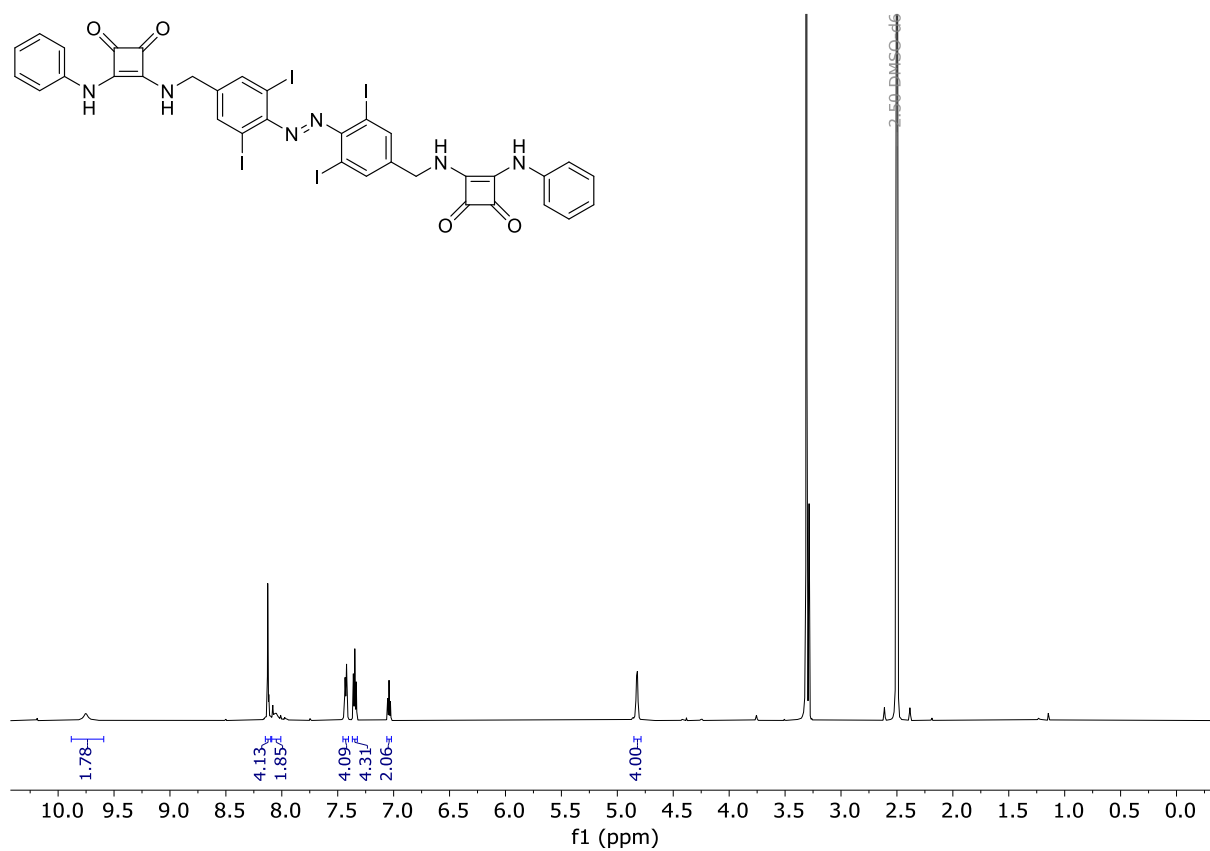


Figure S9. ^1H NMR Spectrum of **I4-sq** (DMSO- d_6 , 298 K).

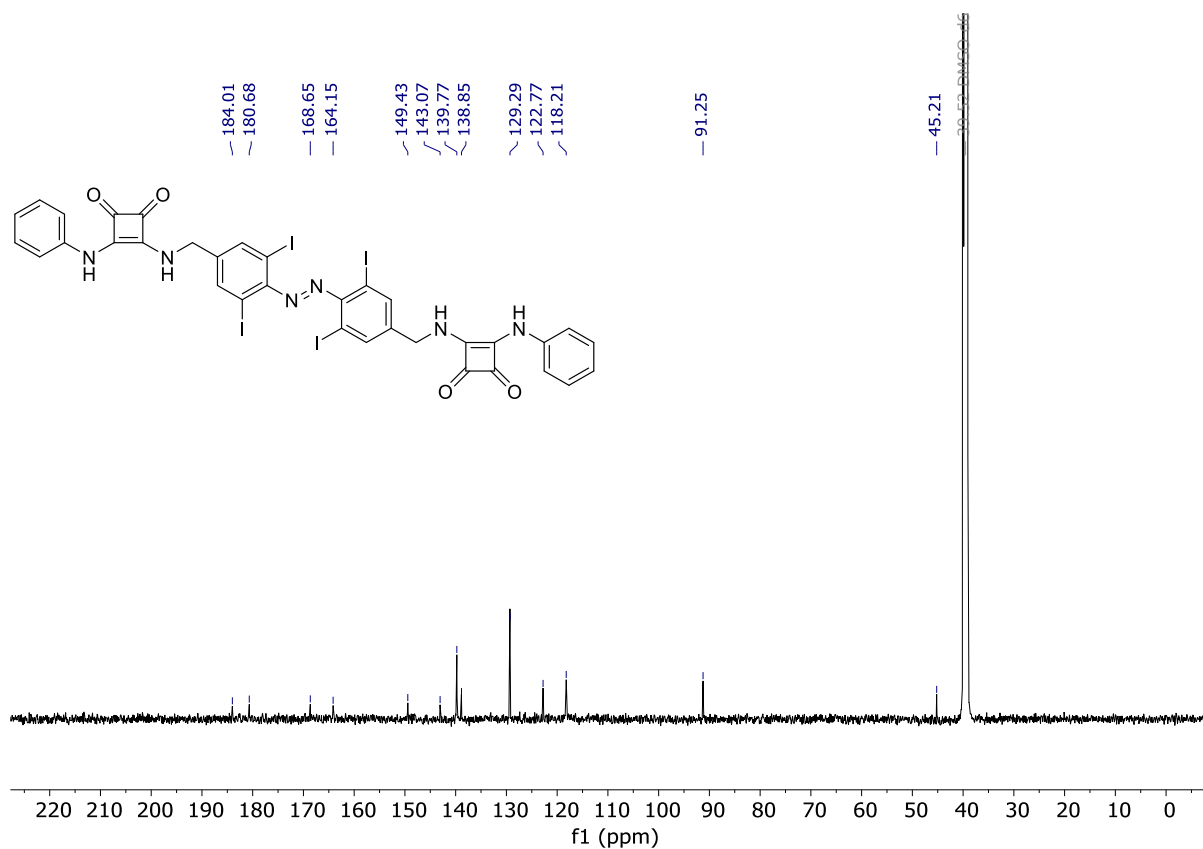


Figure S10. ¹³C NMR Spectrum of **4-sq** (DMSO-*d*₆, 298 K).

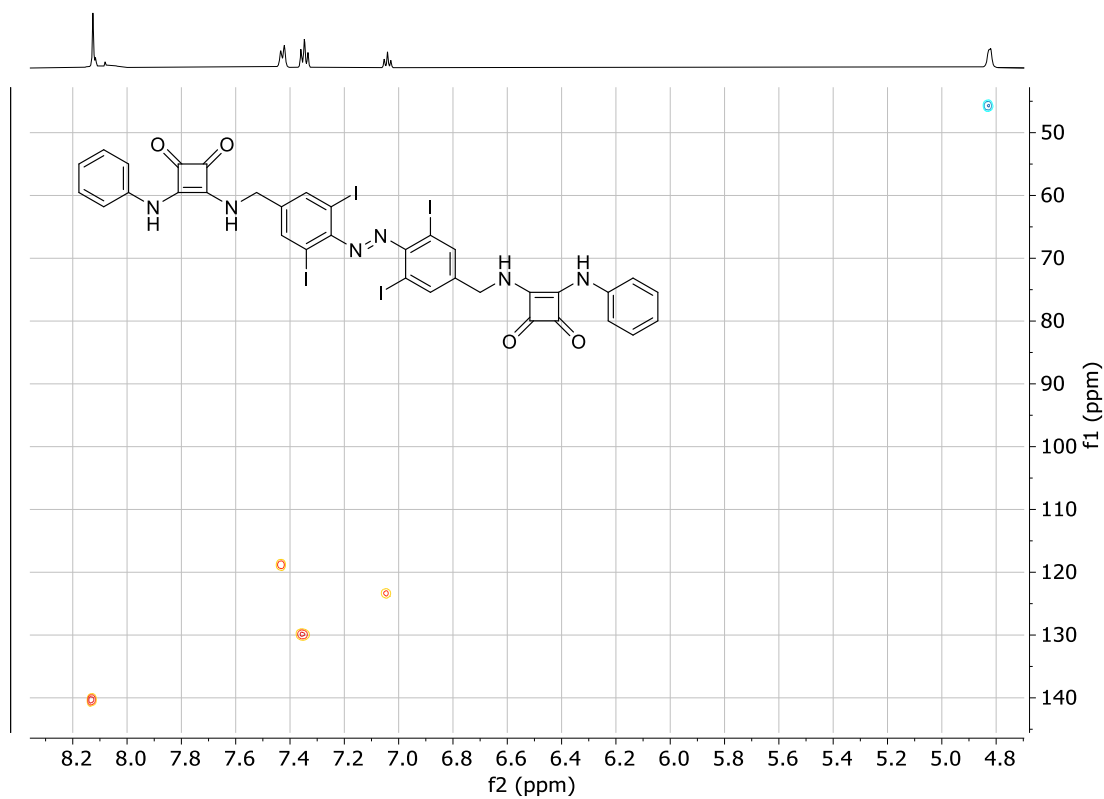


Figure S11. HSQC NMR Spectrum of **4-sq** (DMSO-*d*₆, 298 K).

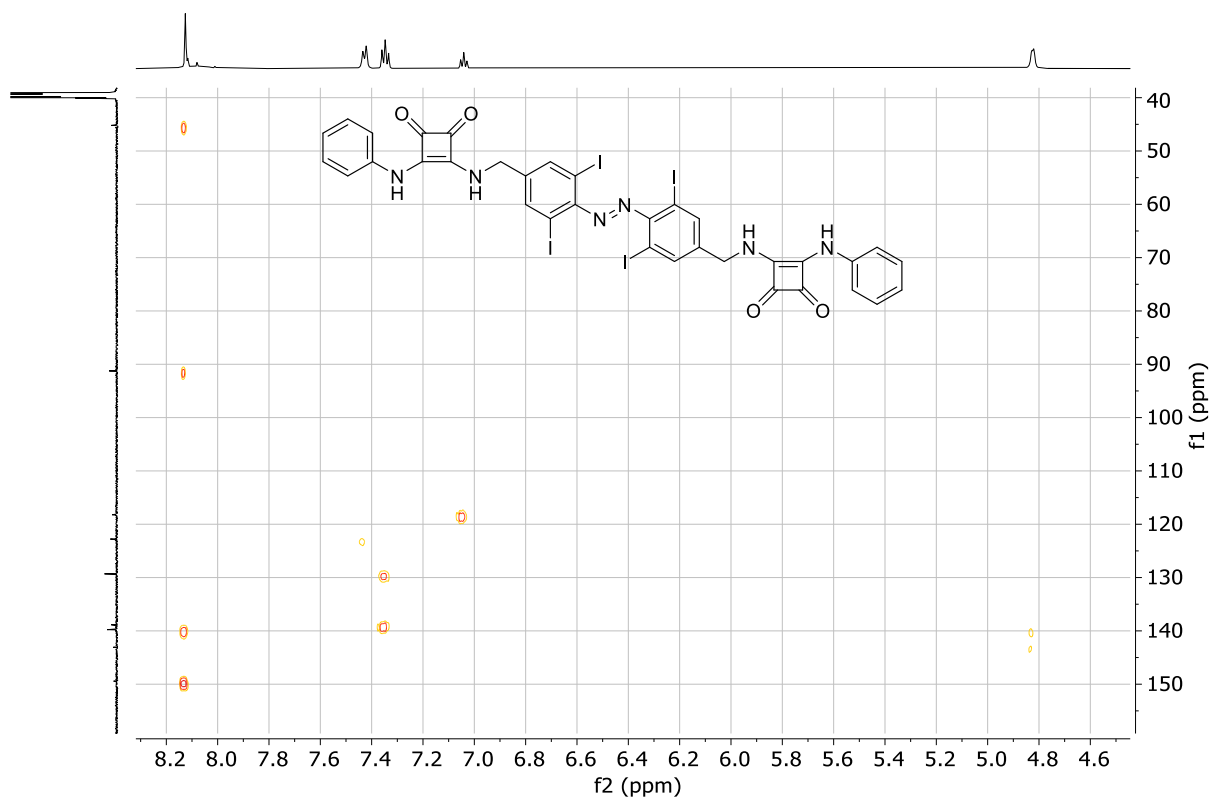


Figure S12. HMBC NMR Spectrum of **I4-sq** (DMSO- d_6 , 298 K).

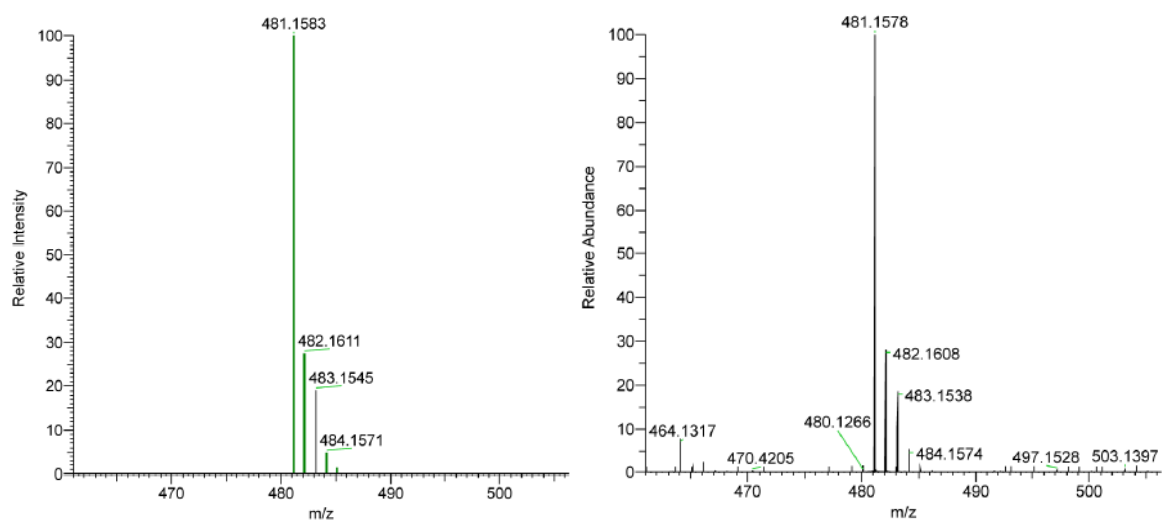


Figure S13. Predicted (left) and observed (right) HRMS spectra for **S4-NH₂**

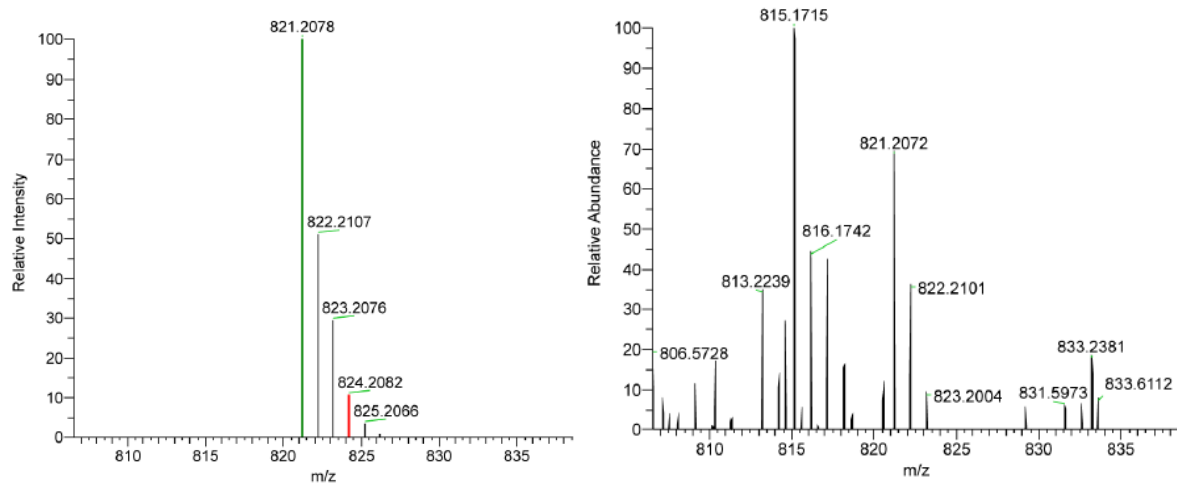


Figure S14. Predicted (left) and observed (right) HRMS spectra for **S₄-sq**

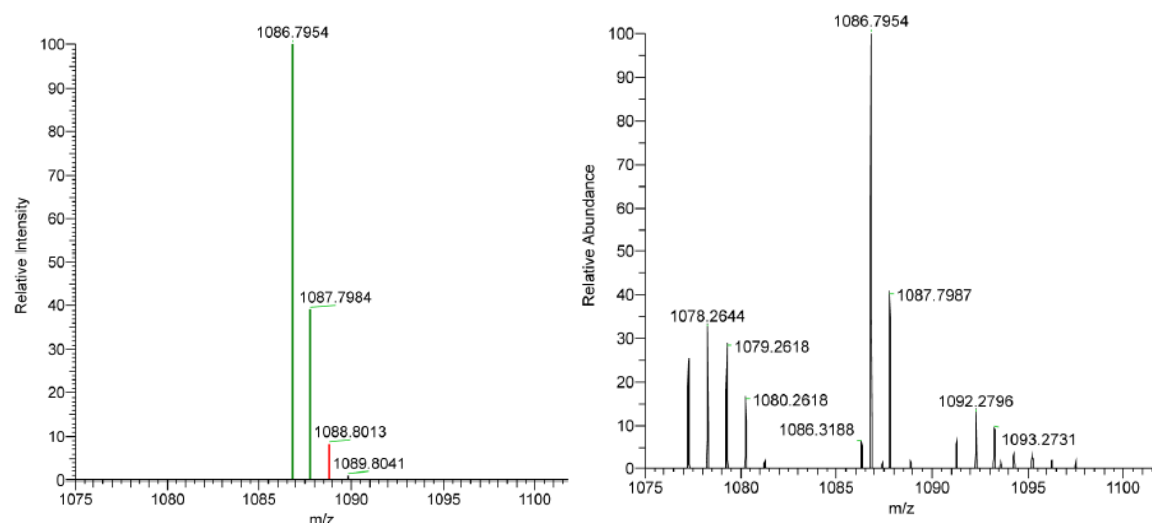


Figure S15. Predicted (left) and observed (right) HRMS spectra for **I₄-sq**

3 Photo-switching: Half-Life Determination and UV-Vis spectra

Photo-irradiation of liquid samples was carried out using Thorlabs high-power mounted LEDs (models M625L4 (red, 625 nm, 920 mW); M590L4 (Amber, 590 nm, 300 mW)).

Half-lives were determined by UV-Vis spectroscopy by irradiating the sample inside the spectrometer and following a single wavelength for the compound over time (Figure S16).

Data was fitted using Origin Pro using an exponential decay model to determine t_1 (Equation S1). The half-life ($\tau_{1/2}$) for the thermal relaxation was determined using Equation S2.

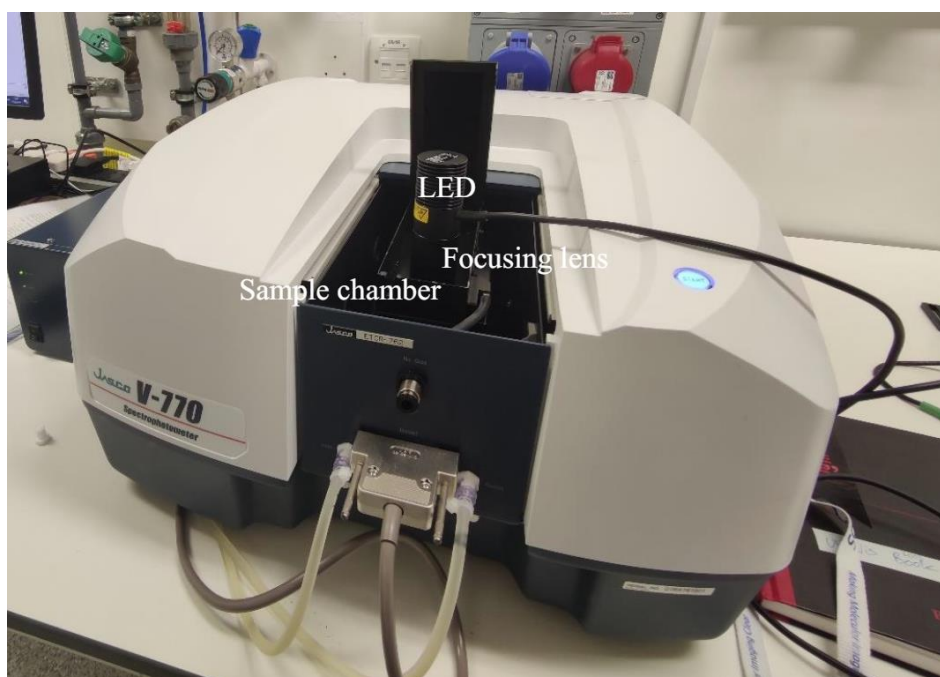


Figure S16. Experimental setup for in-situ switching

$$y = A_1 e^{\frac{-x}{t_1}} \text{ (S1)}$$

$$\tau_{1/2} = t_1 \ln 2 \text{ (S2)}$$

All UV-vis spectra were determined in DMSO solution. Extinction coefficients were determined by recording a UV-vis spectra for the E isomer at 10, 20, 30, 40 μM in DMSO respectively. The absorbance at the maximum of the $\pi - \pi^*$ transition of the E-isomers was plotted against concentration (Beer Lambert plot) to determine the molar extinction coefficient ϵ . For each fast relaxing compound, the E isomer sample at 40 μM was irradiated with the appropriate wavelength of light to generate the photostationary state, and another spectrum was run. This spectrum was normalised to units of ϵ and overlaid with the dark (100% E isomer) spectrum

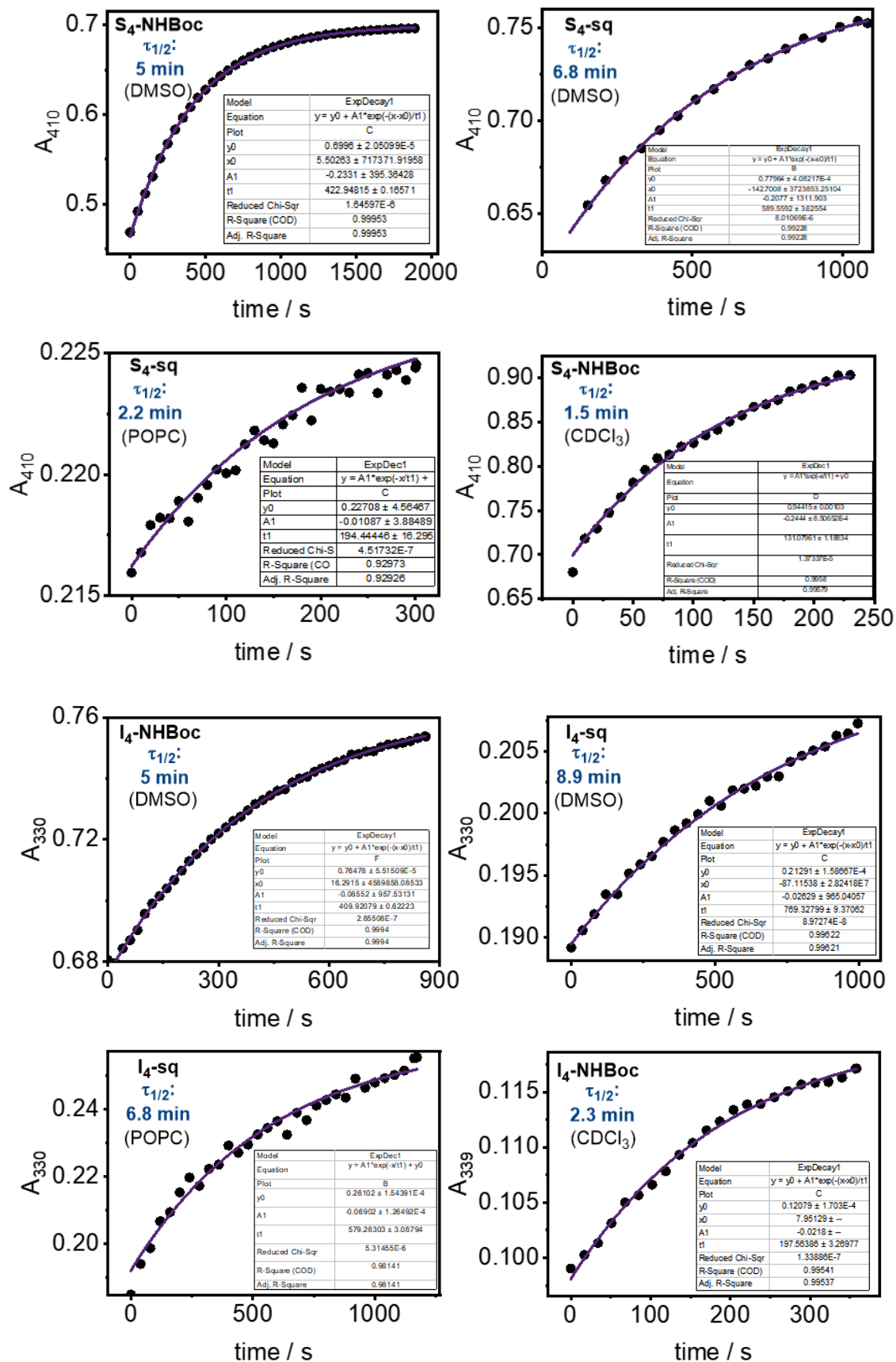


Figure S17. Lifetime plots following UV-Vis absorbance over time after irradiation with 590 nm light (S₄-sq) or 625 nm light (I₄-sq) (rt, 1% transporter relative to lipid for POPC data)

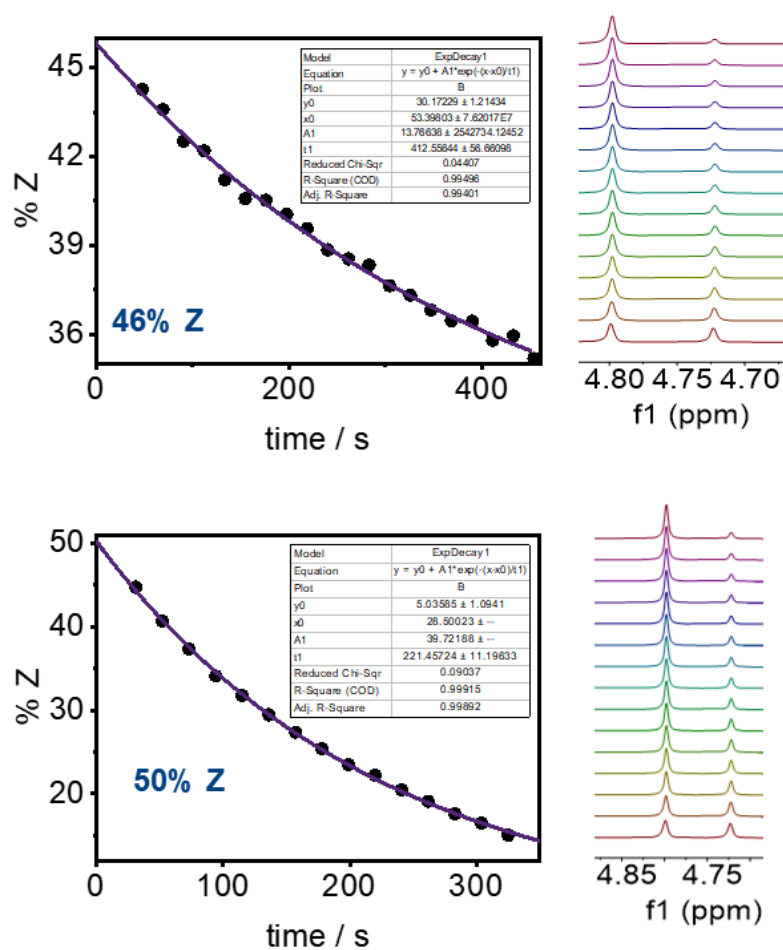


Figure S18. PSS determination for **S₄-NHBoc** [590 nm] (B) **I₄-NHBoc** [625 nm] by generating a PSS-rich sample and running ¹H NMR spectra at known intervals (DMSO-*d*₆, 298 K). The data was fitted to a 1st-order exponential using equation (1) and (2), then extrapolated for t=0 to elucidate the PSS.¹

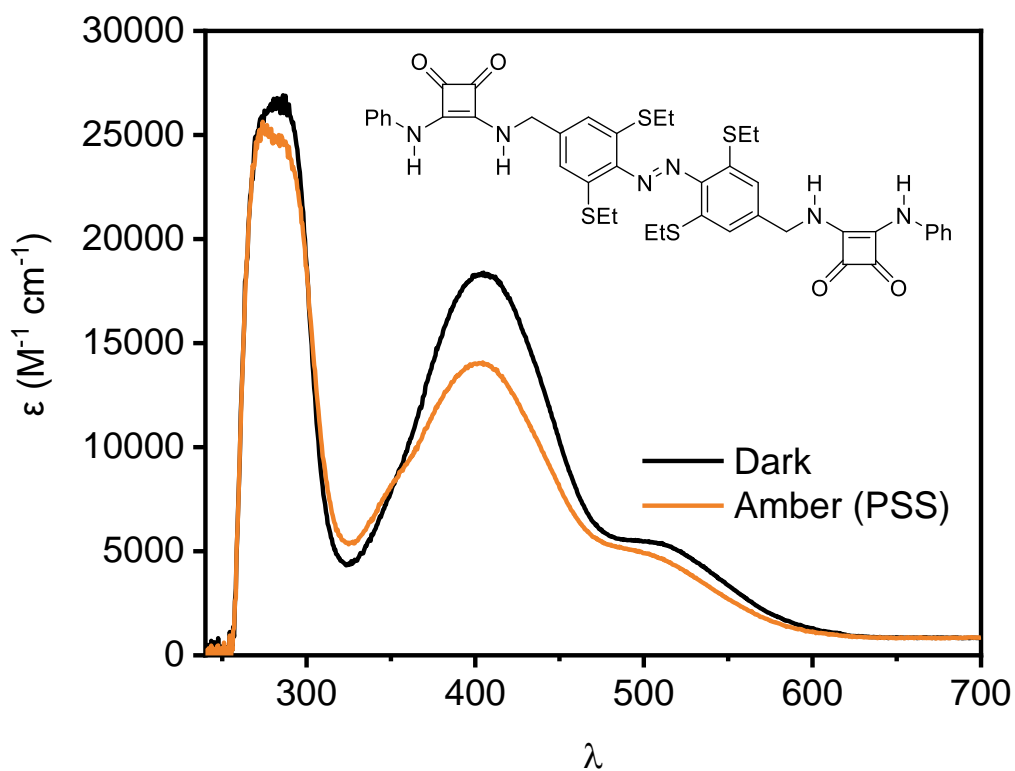


Figure S19. UV-vis Spectrum of **S4-sq** in the dark (100% E) and amber [590 nm] (Z-rich PSS) state (DMSO, rt). Irradiation took place for two minutes.

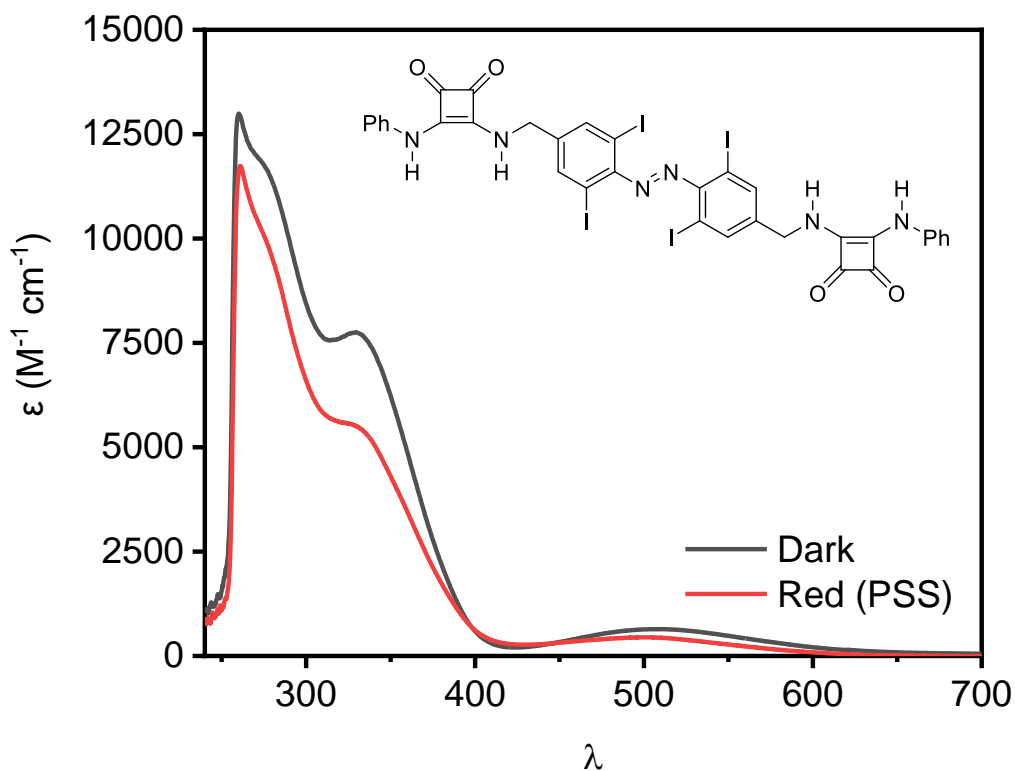


Figure S20. UV-vis Spectrum of **I4-sq** in the dark (100% E) and red [625 nm] (Z-rich PSS) state. (DMSO, rt). Irradiation took place for two minutes.

4 Anion transport studies

Vesicle preparation

A thin film of lipid (1-palmitoyl-2-oleoyl-sn-3-phosphatidylcholine POPC, egg-yolk phosphatidylglycerol EYPG or dipalmitoyl phosphatidylcholine DPPC) was formed by evaporating a chloroform solution under a stream of nitrogen gas, and then under high vacuum for 6 hours. The lipid film was hydrated by vortexing with the prepared buffer (100 mM NaCl, 10 mM HEPES, 1 mM 8-Hydroxypyrene-1,3,6-trisulfonic acid trisodium salt (HPTS), pH 7.0). The lipid suspension was then subjected to 5 freeze-thaw cycles using liquid nitrogen and a water bath (40°C), followed by extrusion 19 times through a polycarbonate membrane (pore size 200 nm) at rt. Extrusion was performed at 50°C in the case of DPPC lipids. Extra-vesicular components were removed by size exclusion chromatography on a Sephadex G-25 column with 100 mM NaCl, 10 mM HEPES, pH 7.0. Final conditions: LUVs (2.5 mM lipid); inside 100 mM NaCl, 10 mM HEPES, 1 mM HPTS, pH 7.0; outside: 100 mM NaCl, 10 mM HEPES, pH 7.0.

Transport assays with HPTS

In a typical experiment, the LUVs containing HPTS (25 μ L, final lipid concentration 31 μ M) were added to buffer (1950 μ L of 100 mM NaCl, 10 mM HEPES, pH 7.0) at 25°C under gentle stirring. A pulse of NaOH (20 μ L, 0.5 M) was added at 20 secs to initiate the experiment. At 80 s the test transporter (various concentrations, in 5 μ L DMSO) was added, followed by detergent (25 μ L of Triton X-100 in 7:1 (v/v) H₂O-DMSO) at 300 secs to calibrate the assay. The fluorescence emission was monitored at $\lambda_{em} = 510$ nm ($\lambda_{ex} = 460/405$ nm). The fractional fluorescence intensity (I_{rel}) was calculated from Equation 34, where R_t is the fluorescence ratio at time t, (ratio of intensities 460 nm / 405 nm excitation) R_0 is the fluorescence ratio at time 77 s, and R_d is the fluorescence ratio after the addition of detergent.

$$I_{rel} = \frac{R_t - R_0}{R_d - R_0} \quad (S3)$$

The fractional fluorescence intensity (I_{rel}) at 290 s just prior to lysis, defined as the fractional activity y , was plotted as a function of the ionophore concentration (x / μ M). Hill coefficients (n) and EC_{50} values were calculated by fitting to the Hill equation (Equation S4),

$$y = y_0 + (y_{max} - y_0) \cdot \frac{x^n}{EC_{50}^n + x^n} \quad (S4)$$

where y_0 is the fractional activity in the absence of transporter, y_{max} is the fractional activity in with excess transporter, x is the transporter concentration in the cuvette.

Exposure of the sample to the excitation beam was minimised by closing the shutter immediately after each measurement, and using a short integration time (0.05 s) / narrow excitation band pass (5 nm). For each compound as the *E* and *Z* isomer, Hill plots were fitted to at-least 8, and up to 12 data points spanning the required concentration range, and each individual concentration was repeated at-least twice and averaged (>16 independent measurements per isomer).

Initial rates were calculated by fitting the first 70 seconds after addition of base pulse to equation (S1), then performing A_1/T_1 to afford the initial rates (s^{-1})

$$y = A_1 e^{\frac{-x}{t_1}} \quad (S1)$$

$$\text{Initial rate (S}^{-1}\text{)} = A_1/T_1 \quad (S5)$$

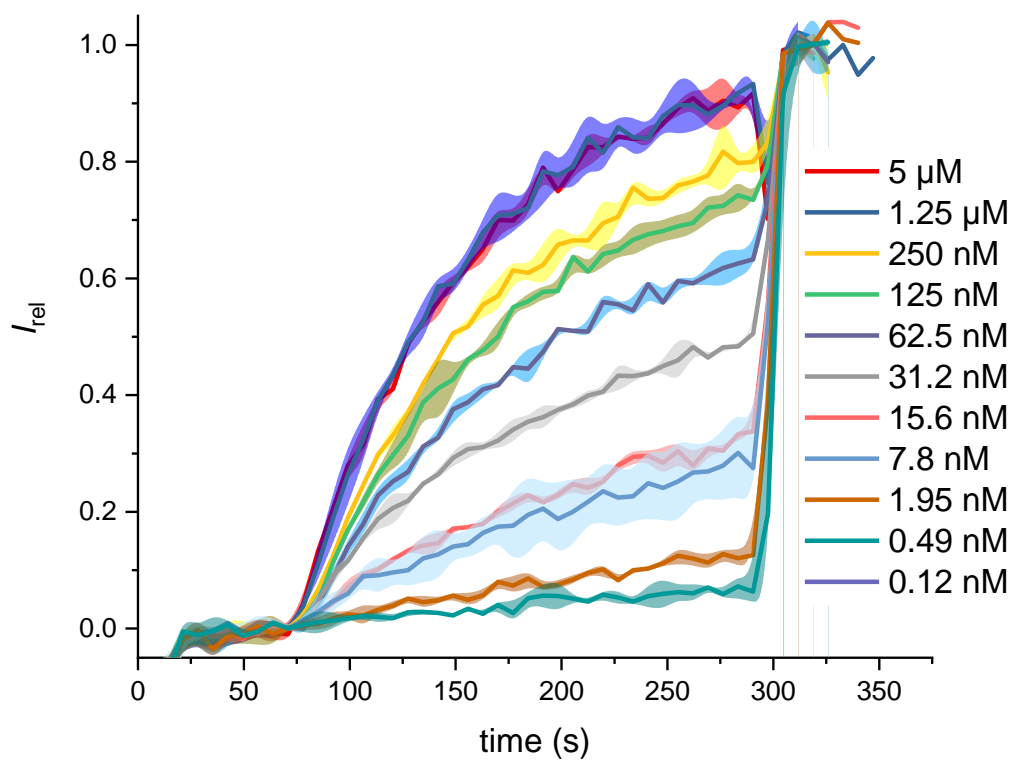


Figure S21. Original data for HPTS assay for (E) - S_4 -sq

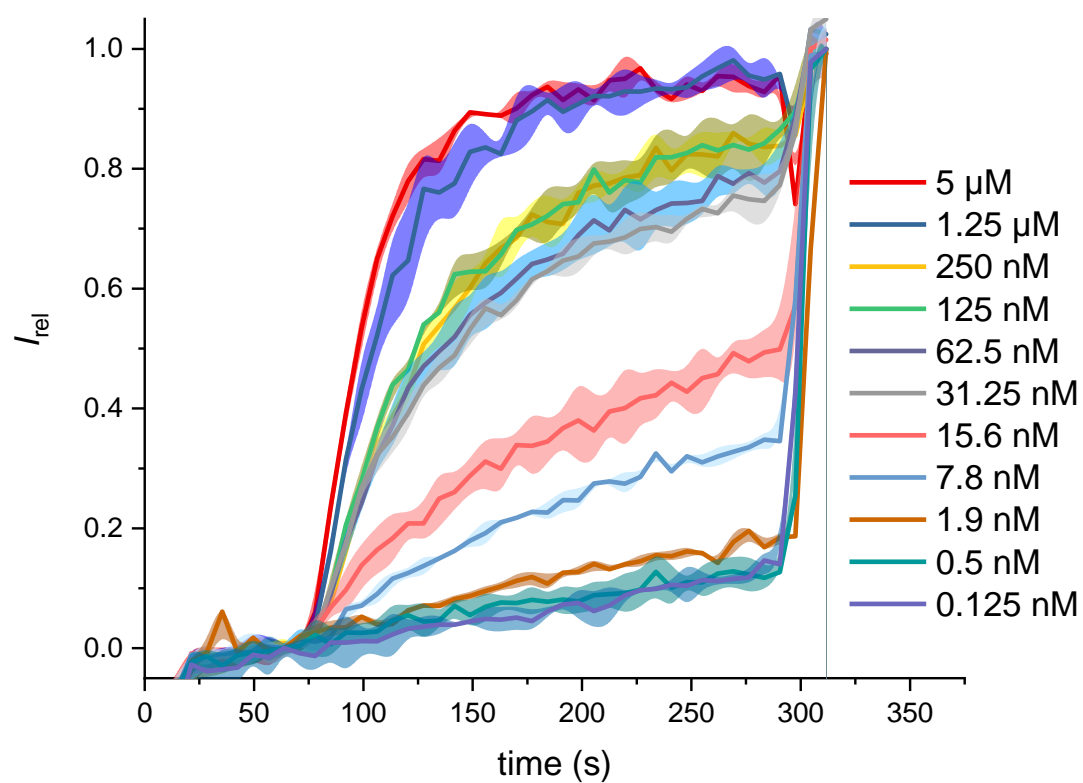


Figure S22. Original data for HPTS assay for amber irradiated (590 nm) S_4 -sq

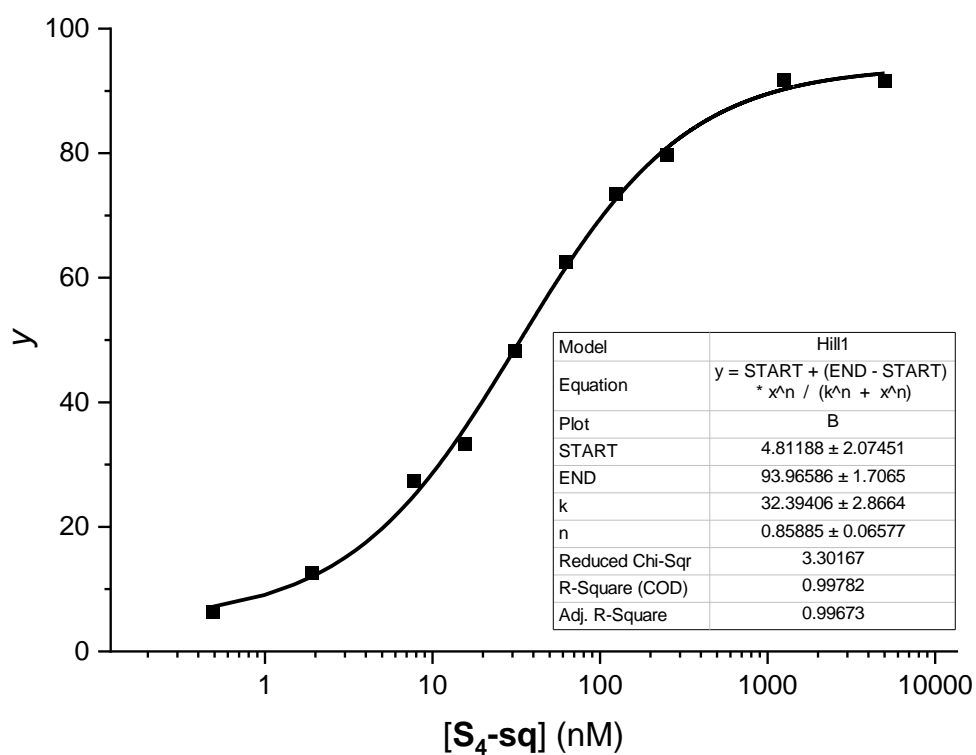


Figure S23. Hill plot for (*E*)-S₄-sq

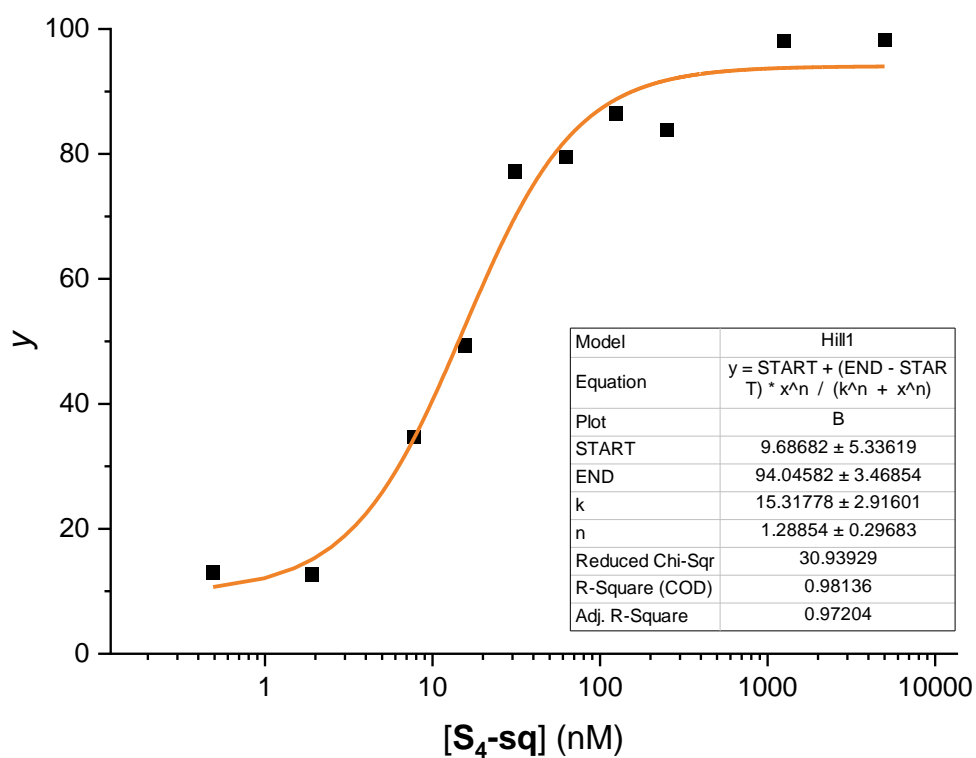


Figure S24. Hill plot for amber irradiated (590 nm) S₄-sq

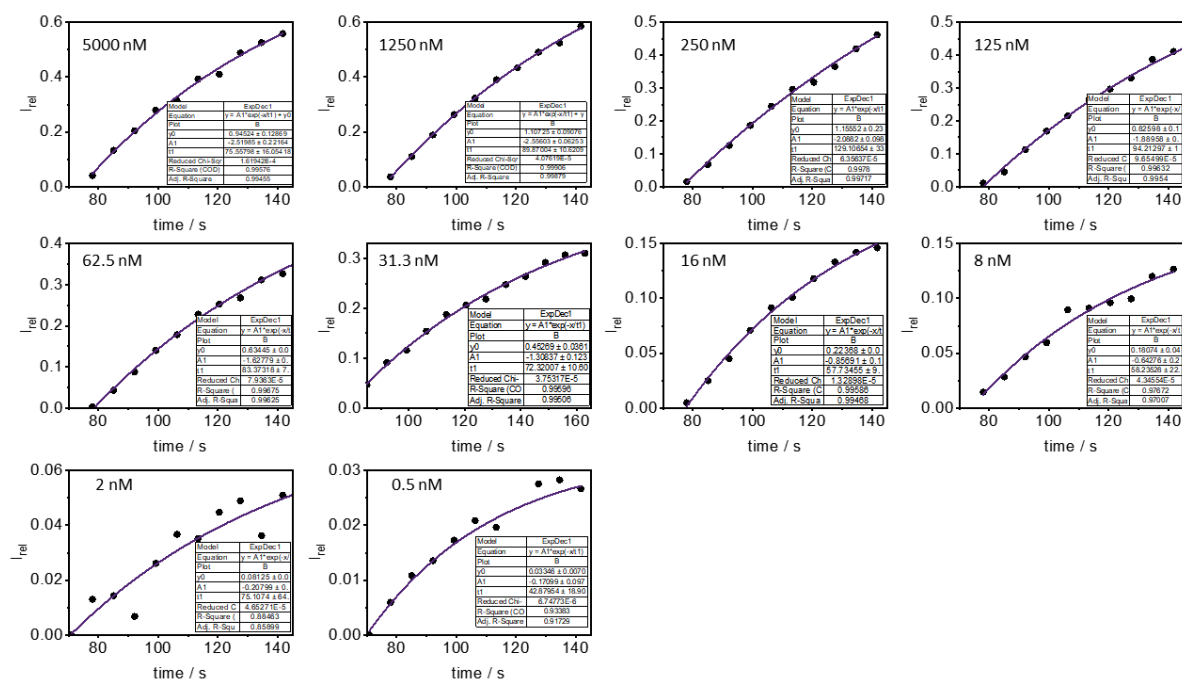


Figure S25. Exponential fits for initial rate analysis of (E)-S₄-sq

Conc. (nM)	5000	1250	250	125	62.5	31.4	16	8	2	0.5
Initial Rate (s ⁻¹)	0.033223	0.028374	0.016172	0.019955	0.019431	0.018114	0.014896	0.010990	0.002663	0.003964

Table S1. Calculated initial rates (A_1/T_1) of (E)-S₄-sq

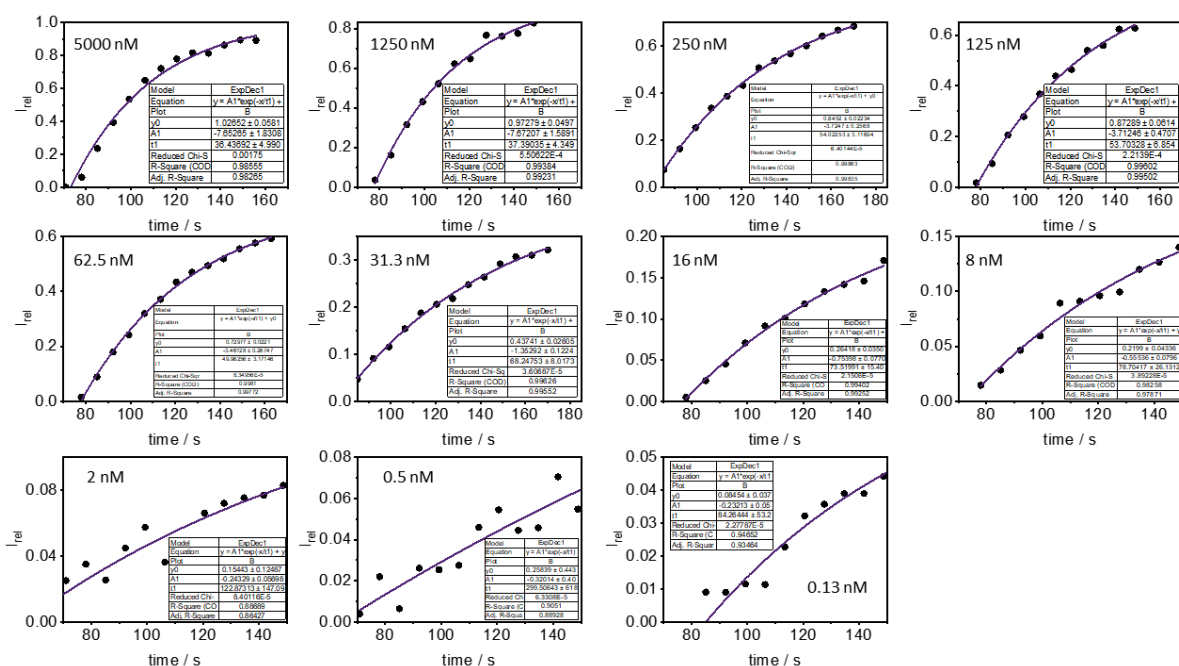


Figure S26. Exponential fits for initial rate analysis of (Z)-S₄-sq

Conc. (nM)	5000	1250	250	125	62.5	31.4	16	8	2	0.5	0.13
Initial Rate (s ⁻¹)	0.209992	0.205135	0.068889	0.069088	0.069255	0.01978	0.010203	0.00704	0.002035	0.001068	0.00273

Table S2. Calculated initial rates (A_1/T_1) of (Z)-S₄-sq

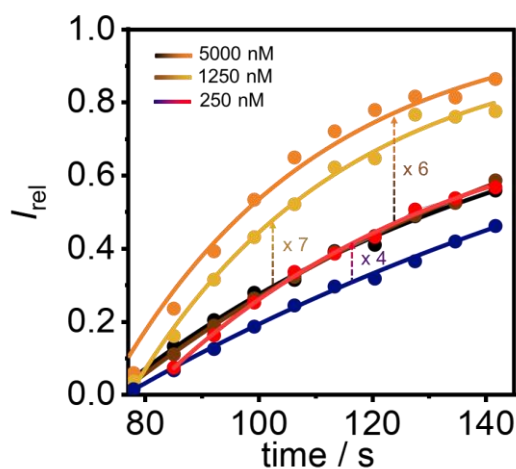


Figure S27. Rate enhancements for S₄-sq upon irradiation with 590 nm LEDs.

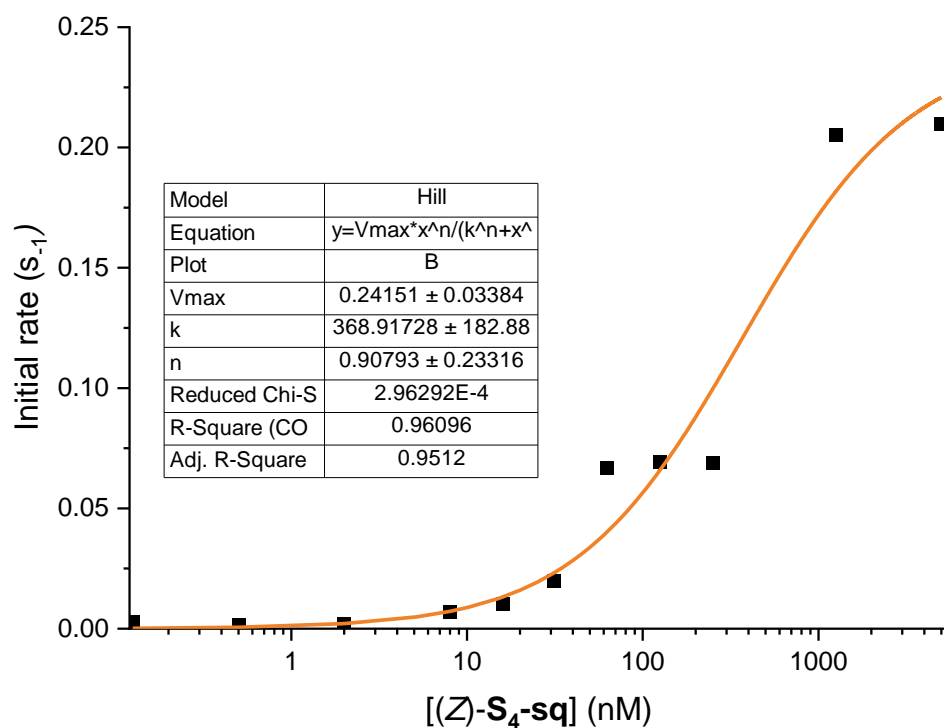


Figure S28. Hill plot for amber irradiated (590 nm) S_4 -sq using initial rate analysis

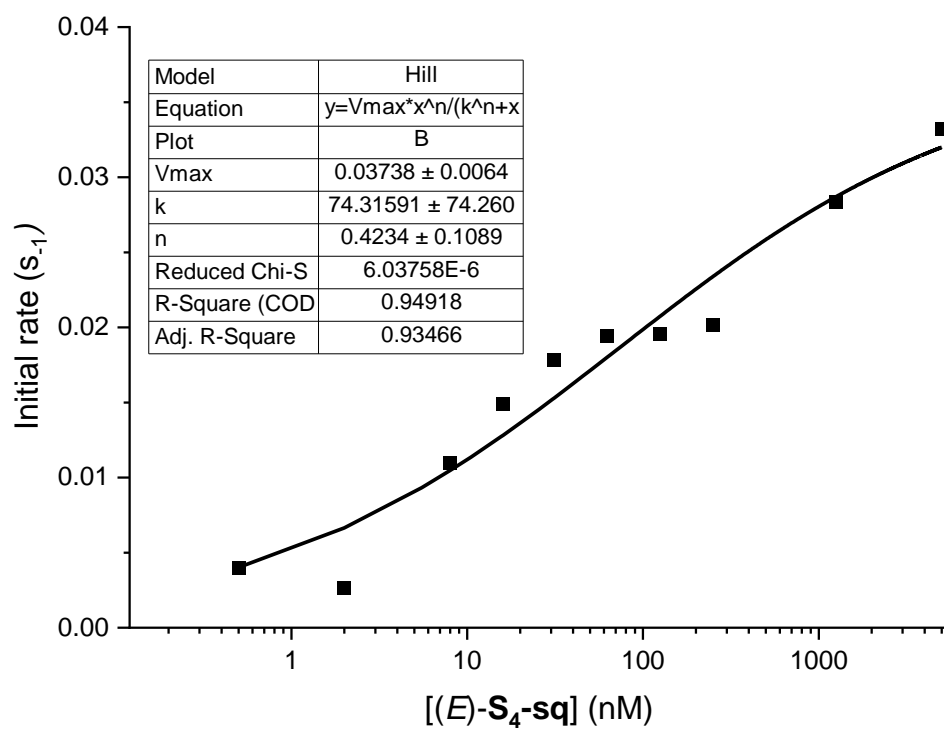


Figure S29. Hill plot for $(E)-S_4$ -sq using initial rate analysis

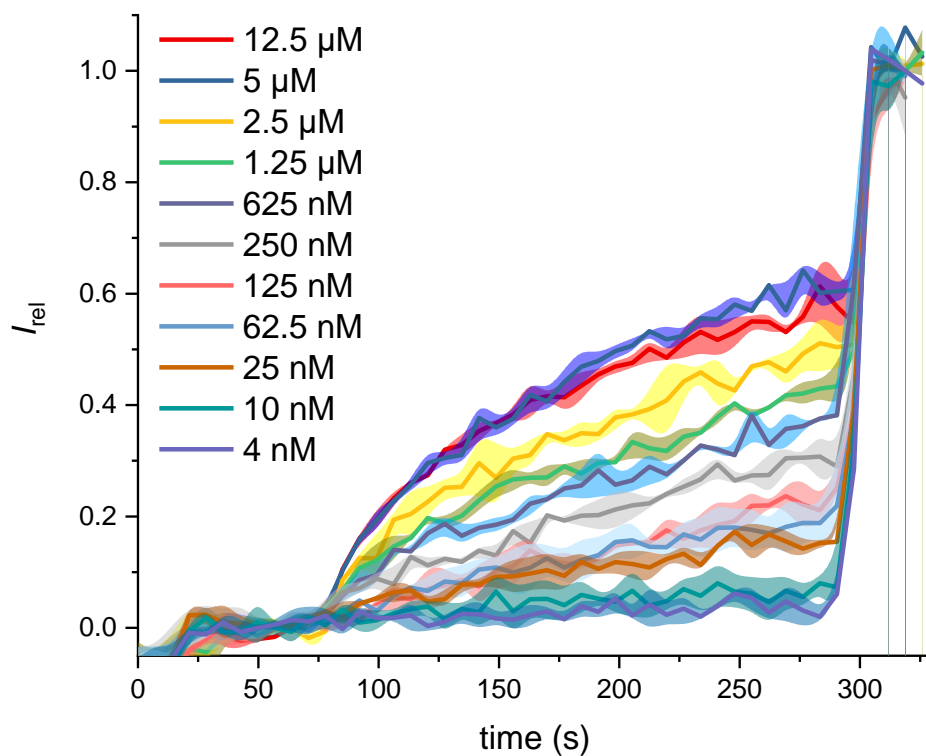


Figure S30. Original data for HPTS assay for (E) -**I₄-sq**

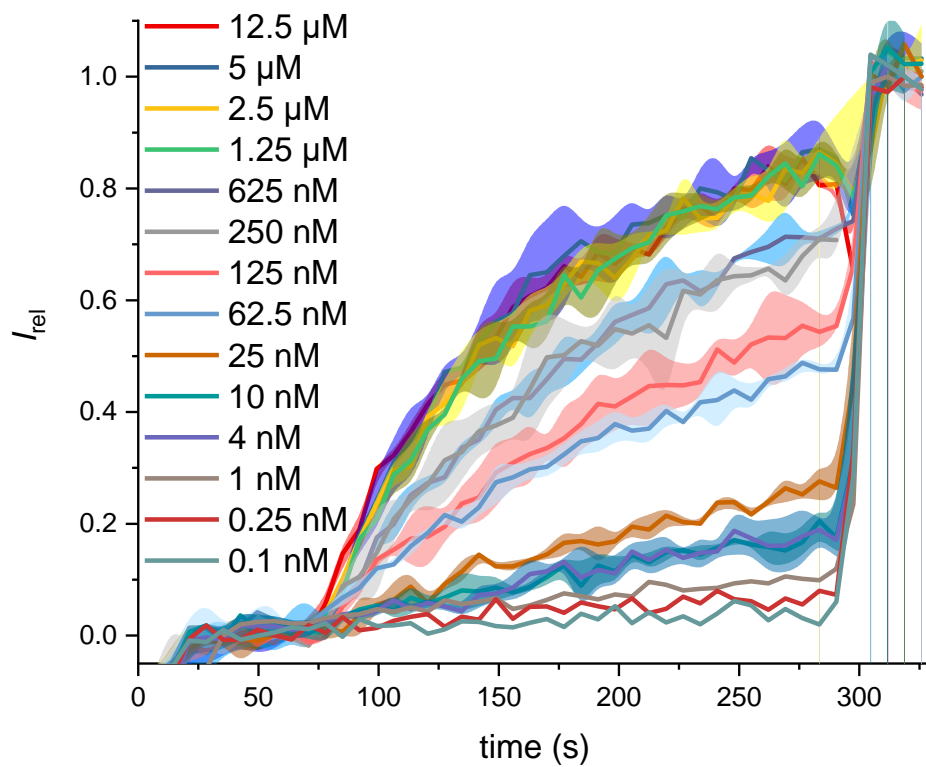


Figure S31. Original data for HPTS assay for red irradiated (625 nm) **I₄-sq**

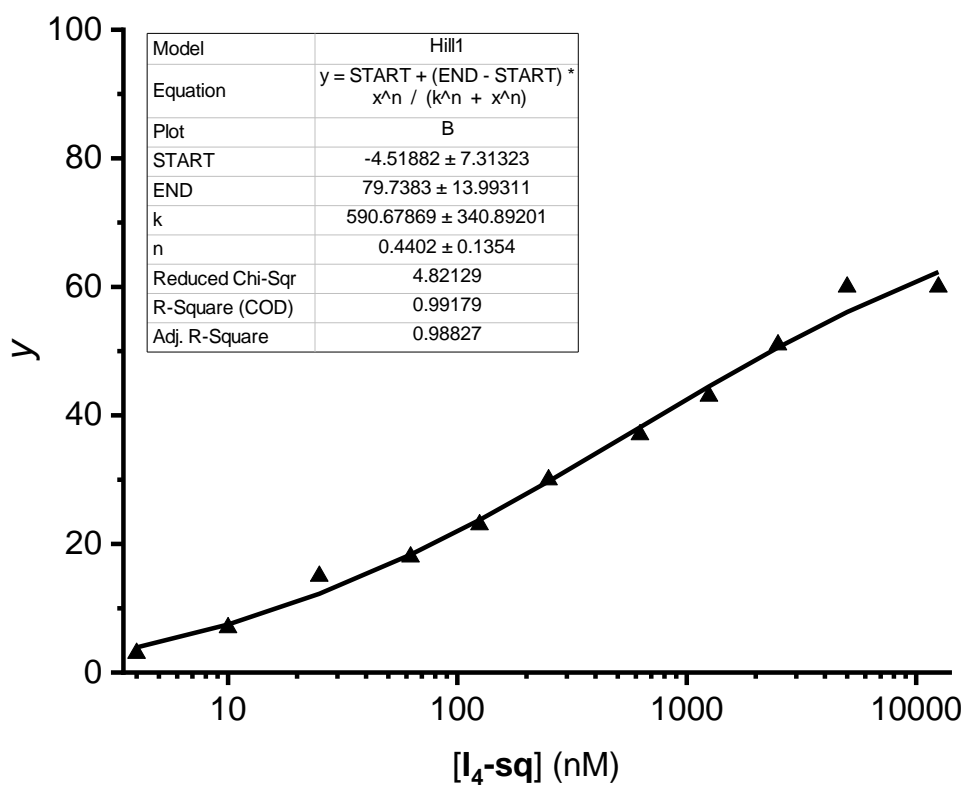


Figure S32. Hill plot for (*E*)-**I₄-sq**

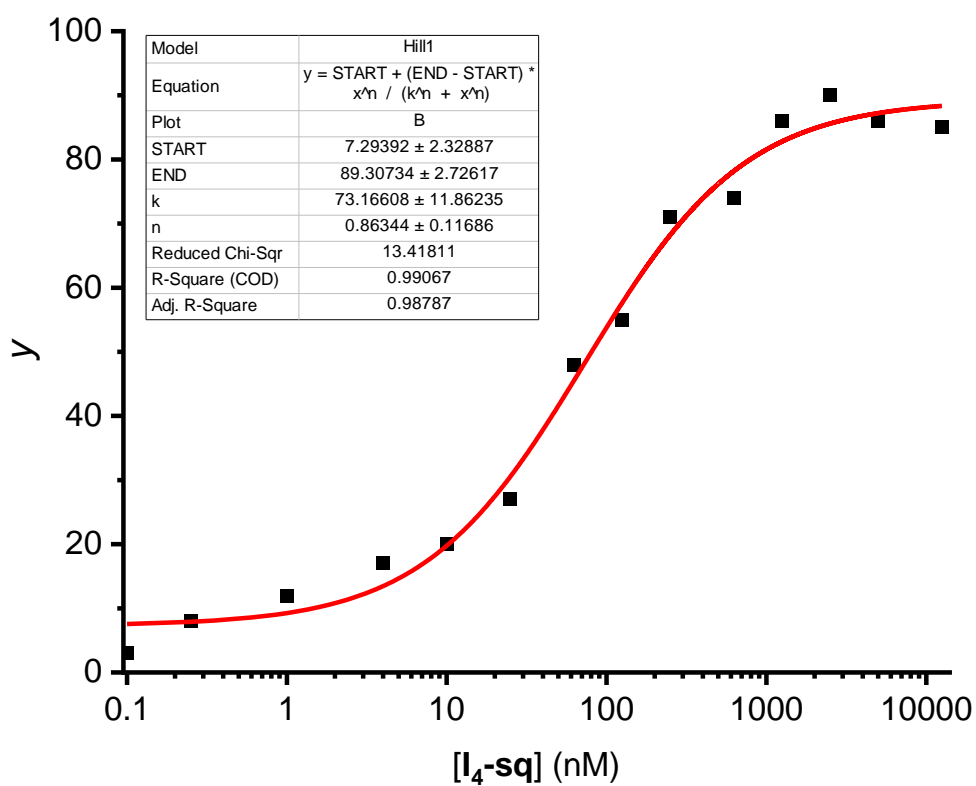


Figure S33. Hill plot for amber red irradiated (625 nm) **I₄-sq**

In-situ Transport assays with HPTS

LUVs containing HPTS (25 μ L, final lipid concentration 31 μ M) were added to buffer (1950 μ L of 100 mM NaCl, 10 mM HEPES, pH 7.0) at 25°C under gentle stirring. A pulse of NaOH (20 μ L, 0.5 M) was added at 20 secs to initiate the experiment. At 80 s, **S₄-sq** (in 5 μ L DMSO) was added. The experiment was recorded using a 510 nm bandpass filter FBH510-10 (Transmission : >90% AT 510 nm, FWHM: 10 nm. Blocking: >OD5 200-497 nm AND 523-1200 nm) – this enables detection of the HPTS emission at 510 nm, but filters the tailing wavelengths of the Thorlabs M590L4 LED). The LED was mounted with a focusing lens (Figure S34A), and placed into the injection chamber of the spectrometer (Figure S34B). The lamp was switched on at $t = 120$ s, and switched off at $t = 320$ seconds.

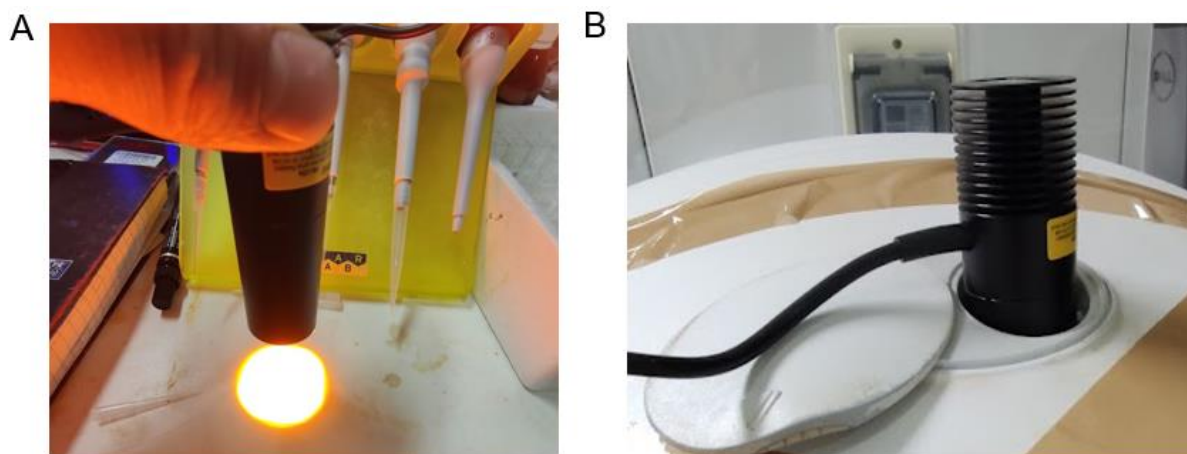


Figure S34 (A) Focussing lens attached to LED (B) Placement of focussing lens + LED in sample chamber of spectrometer.

Photo-thermal responsive ion transport

In a fluorescence cuvette, the LUVs containing HPTS (40 μ L, final lipid concentration 31 μ M) were added to buffer (2890 μ L of 100 mM NaCl, 10 mM HEPES, pH 7.0) at 25°C under gentle stirring. **I₄-sq** (final concentration 66 nM) was added as a DMSO solution to the cuvette. A pulse of NaOH (30 μ L, 0.5 M) was added at 50 secs to create the pH gradient across the lipid membrane to initiate the experiment. Finally, detergent (40 μ L of Triton X-100 in 7:1 (v/v) H₂O-DMSO) was added at 200 secs to calibrate the assay. The fluorescence emission was monitored at $\lambda_{em} = 510$ nm ($\lambda_{ex} = 460/405$ nm). The data recorded immediately after the base pulse was normalised as shown in Figure S35.

The transporter as the *E*-isomer displayed poor ion transport activity. However, when the vesicular solution containing the transporter was photoirradiated using the 625 nm LED for 3 min, a significant enhancement in the ion transport activity was observed due to generation of the *Z*-rich PSS. Subsequently, in order to explore the effect of thermal relaxation on ion transport, the photoisomerized vesicular solution was kept in the dark after irradiation for the state period of time, before addition of the base pulse and measurement of the ion transport activity. Significant deactivation in the ion transport was observed with increasing delay times.

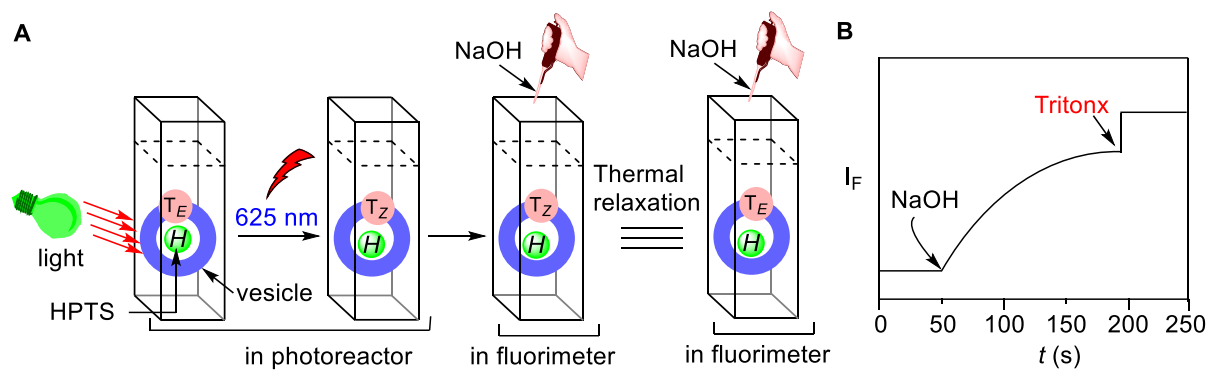


Figure S35. A. Description of photo-thermal responsive ion transport activity of **I₄-Sq** across POPC-LUVs>HPTS. B. Illustration of ion transport kinetics showing normalization window. ‘T’ represents transporter.

5 References

1. A. Kerckhoffs, K. E. Christensen and M. J. Langton, *Chem. Sci.*, 2022, **13**, 11551-11559.
2. A. Kerckhoffs and M. J. Langton, *Chem. Sci.*, 2020, **11**, 6325-6331.